Network architecture and vulnerability of macroalgal epiphyte-host interactions in Caribbean coastal ecosystems: implications for marine conservation

Abdiel Jover [1] *, Asiel Cabrera [1], Ana M. Suárez [2], John Machell [3] and José Lucas Pérez-Lloréns [4]

[1] Departamento de Biología y Geografía, Universidad de Oriente, Patricio Lumumba s/n, Santiago de Cuba, Cuba, CP 90 500.

[2] Centro de Investigaciones Marinas, Universidad de La Habana, Calle 16, No. 114, e/ 1ra y 3ra, Miramar, La Habana, CP 11300.

[3] Pennine Water Group, University of Sheffield, Sir Frederick Mappin Building, Mappin Street, Sheffield, S1 3JD, United Kingdom.

[4] Instituto Universitario de Investigación Marina (INMAR), Universidad de Cádiz (Campus Universitario de Puerto Real, 11510-Puerto Real, Cádiz, Spain.

*Corresponding author: ajover@uo.edu.cu (Abdiel Jover)

Running title: Epiphyte–host network vulnerability in Cuban coastal ecosystems

ORCID ID

Abdiel Jover: https://orcid.org/0000-0002-2040-682

Asiel Cabrera: https://orcid.org/0000-0002-8858-033

Ana M. Suárez: https://orcid.org/0000-0001-7399-3929

John Machell: https://orcid.org/0000-0001-5520-1473

José Lucas Pérez Lloréns: https://orcid.org/0000-0003-2813-1443

Highlights

1. First bipartite network of macroalgal epiphyte–host interactions in the Caribbean (396 nodes, 1,089 edges)
2. Betweenness centrality (β = 0.96) outweighs habitat breadth as predictor of host epiphytic richness
3. The network fragments after removing only 14.6% of hosts targeted by betweenness centrality
4. *Rhizophora mangle* and *T. testudinum* identified as structurally irreplaceable engineer hosts
5. A new Integrated Vulnerability Index (V_{total}) prioritises modules for marine conservation action

ABSTRACT

Background and Aims

Tropical coastal marine ecosystems depend critically on macroalgal epiphyte–host interaction networks to sustain biodiversity, primary production, and ecosystem services, yet the architecture and vulnerability of these networks remain poorly characterised in the Caribbean. This study aimed to characterise the topological structure of the epiphyte–host interaction network in Cuba's coastal marine ecosystems, model the ecological determinants of epiphytic richness, quantify niche overlap among hosts, assess structural robustness to host species loss, and develop an Integrated Community Vulnerability Index (V_{total}) to guide conservation prioritisation.

Methods

A bipartite network was constructed from a comprehensive synthesis database comprising 62 host taxa and 321 epiphytic macroalgal species across eight coastal habitat types. Network topology was analysed using degree distribution modelling, Louvain community detection, and centrality metrics. Host habitat distributions were inferred via a hierarchical Bayesian model validated against 18 hosts of known distribution. Epiphytic richness was modelled using a Bayesian negative binomial regression with inferred habitat breadth and betweenness centrality as predictors. Niche overlap was assessed with Jaccard similarity and Monte Carlo permutation tests. Structural robustness was evaluated through sequential host-removal simulations under three strategies. V_{total} was calculated by integrating habitat environmental vulnerability with network-structural irreplaceability.

Key Results

The network comprised 396 nodes and 1,089 edges (connectance = 0.0315), with degree distribution best described by a truncated power law. Eighteen modules were identified (Q = 0.424). Betweenness centrality (β = 0.957) was a stronger predictor of epiphytic richness than habitat breadth (β = 0.524). Overall Jaccard similarity was extremely low (mean = 0.027), indicating high functional complementarity. Targeted host removal caused network fragmentation after only 14.6% of hosts were removed, versus 64.6% under random removal. *Rhizophora mangle*, *Thalassia testudinum*, and *Digenea simplex* emerged as irreplaceable structural hubs. Mangrove module M9 attained the highest V_{total} (4.264).

Conclusions

The epiphyte–host network is architecturally efficient yet ecologically fragile, with a disproportionate dependence on a small set of engineering host species whose loss would trigger non-linear cascades of secondary epiphyte extinctions and ecosystem service degradation. The

Integrated Vulnerability Index provides a transferable, interaction-based framework for conservation prioritisation in tropical marine systems facing accelerated environmental change.

INTRODUCTION

Tropical coastal marine ecosystems rank among the most productive and biodiverse habitats on Earth. The ecological integrity of these ecosystems underpins essential ecosystem services, including biodiversity maintenance, provision of fishery resources, coastal protection, and carbon sequestration (Duarte *et al.* 2020; Hanley *et al.* 2024). In these ecosystems, macroalgae fulfill multifaceted ecological roles as primary producers, ecosystem engineers, and providers of three-dimensional habitat for a vast diversity of associated organisms (Teagle *et al.* 2017; Salland *et al.* 2024). However, the ecological function of macroalgae cannot be understood in isolation; they are central components of ecological interaction networks that shape benthic community structure and functioning.

Epiphytism, defined as the growth of autotrophic organisms on living autotrophic substrates (hosts) without a direct parasitic relationship, constitutes one of these fundamental interactions (Potin 2012; Álvarez-Álvarez *et al.* 2020). In the case of macroalgae, epiphyte-host relationships modulate community dynamics, biogeochemical cycles, and ecosystem resilience (Korlević *et al.* 2021). The composition and diversity of the epiphyte assemblage depend on host-intrinsic factors, such as longevity, surface area, morphological architecture, and secondary metabolism, as well as environmental conditions (Jover, Ramos, *et al.* 2020; Álvarez-Álvarez *et al.* 2020; Quiroz-González *et al.* 2023; Gossard 2024). Despite their ecological relevance, these associations in tropical marine environments tend to exhibit less specificity than those in terrestrial systems, suggesting assembly dynamics governed by complex processes that require integrative analytical frameworks for their correct interpretation (Harder 2008; Díez *et al.* 2012; Diez *et al.* 2013).

The concept of ecosystem engineer species, which modulate the availability of resources for other species by causing physical changes in the habitat, is particularly heuristic for understanding the structural role of host macroalgae (Jones *et al.* 1996; Thomsen *et al.* 2018). Host macroalgae act as engineers by creating three-dimensional microhabitats that facilitate the settlement and development of epiphytic communities, thus generating habitat cascades that amplify local and regional biodiversity (Teagle *et al.* 2017). The loss of these engineer species can trigger disproportionate effects on ecosystem structure and function, especially if they occupy critical topological positions within the network of interactions (Valls *et al.* 2015; Li *et al.* 2025).

Consequently, elucidating the architecture of epiphyte-host networks and the functional irreplaceability of key species is a priority for management and conservation.

Ecological network theory provides an appropriate conceptual and methodological framework for analyzing the structure and dynamics of complex communities. This approach allows us to identify emerging organizational patterns, such as modularity and heterogeneous connectivity distributions, as well as to detect key species and structural vulnerabilities (Bascompte and Jordano 2013; Bascompte 2019; Domínguez-García and Kéfi 2024). In marine ecosystems, network analysis has enabled to identify key species using centrality metrics, assess structural robustness to disturbances through node removal simulations, and predict secondary extinction cascades (Jones *et al.* 2024; Li *et al.* 2025). However, the application of these methodologies to epiphyte-host interaction networks in tropical macroalgae has been limited (Cabrera *et al.* 2024), which constitutes a significant knowledge gap.

The Caribbean and Cuba in particular, constitutes an ideal region for studying epiphyte–host networks. The region is characterized by a high habitat heterogeneity, coral reefs, seagrass beds, mangroves, rocky and sedimentary bottoms, and a considerable diversity of macroalgae (Jover, Ramos, *et al.* 2020; Quiroz-González *et al.* 2023; Suárez *et al.* 2023). Nevertheless, these ecosystems face escalating threats from climate change and anthropogenic pressures. Climate models project increases in sea surface temperature, ocean acidification, more frequent coral bleaching events, intensification of tropical storms, and sea level rise, with impacts on biodiversity and human well-being in the region (Mcleod *et al.* 2010; Micheli *et al.* 2013; Valderrama *et al.* 2018; O Guzmán *et al.* 2023). Recent studies document the differential vulnerability of these ecosystems, with coral reefs and seagrass beds being particularly susceptible (Chollett *et al.* 2010; van Tussenbroek *et al.* 2017). The projected loss of critical habitats, with predictions of 83-88% decline in coral reefs by 2100 under realistic climate scenarios, underscores the urgency of developing predictive tools and prioritization frameworks for conservation (Freeman *et al.* 2013; H Guzmán *et al.* 2023).

The integration of Bayesian statistical models with ecological network analysis provides an appropriate framework for addressing complex questions about the structure, function, and vulnerability of communities (Schoolmaster *et al.* 2020; White *et al.* 2024). Hierarchical Bayesian models allow for the explicit incorporation of uncertainty, the integration of multiple sources of information, and the simultaneous estimation of parameters at different ecological

scales (Qian *et al.* 2009; White *et al.* 2024). In the marine context, these approaches have demonstrated their superiority for the analysis of observational data, particularly in the presence of nested effects, complex spatial variability, and overdispersion (Qian *et al.* 2009; Granata *et al.* 2024). Complementarily, Bayesian networks are emerging as promising tools for inferring ecological interactions from spatial and temporal co-occurrence data, facilitating network reconstruction when direct interaction data are limited (Aderhold *et al.* 2012; Trifonova *et al.* 2014).

Despite these methodological advances, significant gaps remain in our understanding of epiphyte-host networks in tropical marine ecosystems. First, there is a lack of integrative analyses that connect the topological structure of networks (*e.g.*, modularity, centrality) with underlying ecological processes (*e.g.*, host niche breadth, association specificity) across multiple scales. Second, most studies on epiphytism have focused on taxonomic characterizations and spatial distributions, without exploring the implications of network architecture for ecosystem vulnerability and conservation priorities. Third, there is a critical need to develop integrated vulnerability indices that combine the environmental exposure of habitats with the structural role of host species within interaction networks, thereby facilitating the translation of scientific findings into concrete management actions.

To address these gaps, this study aims to characterize the architecture of the epiphyte-host interaction network in Cuba's coastal marine ecosystems. Specifically, it aims to: (i) analyze the topological structure of the network, including its modular organization, connectivity distribution and specialization patterns; (ii) model the ecological determinants of epiphyte richness, evaluating the effect of habitat breadth and the structural centrality of the host; (iii) quantify niche overlap patterns among hosts based on their position in the network; (iv) to evaluate the structural robustness of the network in the face of sequential removal of host species under different disturbance scenarios; and (v) to develop an Integrated Community Vulnerability Index that combines the environmental vulnerability of habitats with the structural irreplaceability of host species to identify conservation priorities

The research revolves around the following main question: How is the network of epiphyte-host interactions organized in Cuba's coastal marine ecosystems, and which host species, due to their critical structural role, could disproportionately compromise the integrity of the network and the provision of ecosystem services in the event of loss? The following hypotheses are derived from

this question: (H1) The epiphyte-host network will exhibit significant modular organization with a heterogeneous distribution of connectivity, where a few host species will act as hubs with high epiphyte richness (Bascompte and Jordano 2013; Domínguez-García and Kéfi 2024). (H2) The richness of epiphytes associated with a host will be positively related to its habitat breadth and structural centrality in the network (Álvarez-Álvarez *et al.* 2020; Gouveia *et al.* 2021; Gossard 2024). (H3) (H3) Hosts with greater centrality and epiphyte richness will harbor less unique epiphyte assemblages (greater niche overlap), while peripheral hosts will sustain more unique assemblages. (H4) The network will show greater vulnerability (accelerated fragmentation) to targeted removal of species based on their centrality than to random removal, evidencing a critical dependence on key engineer species (Dunne *et al.* 2002; Thompson 2006; Gribben *et al.* 2017). (H5) Modular communities with greater integrated vulnerability will be those that combine environmentally vulnerable habitats with the presence of host species with high structural irreplaceability.

This study constitutes the first comprehensive analysis of epiphyte-host networks that integrates Bayesian modelling, topological network analysis, structural robustness assessment, and the development of vulnerability indices applied to conservation. The results will contribute to the general theory of marine ecological networks, provide critical information on key engineer species in Cuban coastal ecosystems, and generate transferable tools for conservation prioritization in other tropical marine systems facing accelerated environmental change.

MATERIALS AND METHODS

Study Design and Conceptual Framework

This research uses data derived from a comprehensive systematic review of epiphyte-host associations in coastal marine ecosystems in Cuba (Jover, Ramos, *et al.* 2020; Jover, Cabrera, *et al.* 2020). The design is based on a retrospective observational approach to data synthesis and adopts a hierarchical and multiscale perspective (Figure 1). This perspective is consistent with established theoretical frameworks that recognize that ecological processes and patterns are highly dependent on the scale of observation and the level of biological organization considered (Levin 1992; Wiens and Donoghue 2004). This conceptual framework considers three interdependent ecological levels: (i) coastal marine habitats, (ii) host macroalgae communities, and (iii) epiphytic macroalgae assemblages.

The framework integrates bottom-up processes—physical and biological habitat conditions that regulate host availability and distribution—and top-down processes—emergent effects of interaction network structure on community stability and organization (Polis *et al.* 2000; Bascompte and Jordano 2007). This approach allows for the simultaneous evaluation of spatial, relational, and probabilistic patterns, linking the architecture of biological interactions with the stability of the ecosystem services provided by these assemblages, including the provision of structured habitat and the maintenance of associated biodiversity (Díaz *et al.* 2006; Tylianakis *et al.* 2010).

Starting Database and Analytical Matrices

The records of epiphytic macroalgae and their hosts are based on the database available at Figshare (Jover, Guerrero, Machell, A M Suárez, and Pérez-Llorens 2026). From this information, two central matrices were constructed, which constitute the main information for the present analyses. The first is the Epiphyte-Habitat matrix (H; 321 × 8), which indicates the presence (1) or absence (0) of each of the 321 species of epiphytic macroalgae in each of the eight recognized types of coastal marine habitats (Table 1). The second is the Host-Epiphyte matrix (A; 130 × 266) documents the presence (1) or absence (0) of a biological association between each of the 130 host taxa and the 321 epiphytes. The 55 species excluded from the analysis did not have complete data on the host species.

The taxonomic nomenclature of both matrices was verified and updated against the World Register of Marine Species (Ahyong *et al.* 2026) using the *taxize* v0.9.100 package in R (Chamberlain *et al.* 2020). This package corrects minor synonymies or nomenclatural updates subsequent to the publication of the base study. Additionally, the validity of the taxa was updated through AlgaBase (Guiry and Guiry 2024).

From the first habitat matrix (H; 321 × 8), where each element H_{ij} represents the presence (1) or absence (0) of epiphyte *i* in habitat *j*. The second was the Interaction Matrix (A; 130 × 321), where each element A_{kj} indicates the presence (1) or absence (0) of the association between host *k* and epiphyte *j*.

For each epiphytic macroalgae i, habitat breadth was estimated as the number of habitats occupied, based on a presence–absence modification of the niche breadth concept proposed by Levin (Levin 1992):

$$B_i = \sum_{j=1}^{8} H_{ij}$$

and the normalized habitat generalism index (G_i^h), expressed as a proportion of the maximum number of possible habitats:

$$G_i^h = \frac{B_i}{8}$$

From matrix A, for each host macroalgae *k*, the epiphyte richness was calculated as:

$$R_k = \sum_{j=1}^{321} A_{kj}$$

Analysis of the Interaction Network

The epiphyte-host association was represented as an undirected bipartite network, where the nodes correspond to species and the edges represent documented interactions. Network analyses were performed using the *igraph* v1.5.1 package in R (Csárdi *et al.* 2023). The following metrics were calculated for each node v. (i) Degree: k(v) = number of direct connections of the node. (ii) Normalized betweenness centrality CB(v): measures the frequency with which a node acts as a bridge in the shortest paths between other pairs of nodes, constituting a standard indicator of the connecting role of a node in the network (Freeman 1977). (iii) Normalized closeness centrality: inverse of the average geodesic distance of the node to all other reachable nodes (Freeman 1977). Global network metrics were also calculated: density, clustering coefficient, average path length (APL), and network diameter (Newman 2010).

The modular structure of the network was identified using the Louvain algorithm (Blondel *et al.* 2008). This is one of the most widely used community detection methods in complex networks due to its computational efficiency and robustness in large networks. The algorithm iteratively maximizes the modularity function Q (Newman and Girvan 2004):

$$Q = \frac{1}{2m}\sum_{ij}\left[A_{ij-\frac{K_I K_j}{2m}}\right]\delta(c_i c_j)$$

Where *m* is the total number of edges, *Aij* are the elements of the adjacency matrix, k_i is the degree of node *i*, and δ (c_i , c_j) = 1 if nodes *i* and *j* belong to the same community.

The cumulative distributions of the number of interactions per species were evaluated by fitting three different models: exponential, power law, and truncated power law (Jordano *et al.* 2003; Olesen *et al.* 2006). To compare the fit between models, the Akaike Information Criterion (AIC)

(Zhang *et al.* 2023) was calculated, following the model selection criteria of Burnham and Anderson (2002). Statistical analyses were performed in the R environment using the *igraph* (Csárdi *et al.* 2023) and *poweRlaw* (Gillespie 2015) packages.

Node Removal Simulation and Robustness Analysis

To assess the structural fragility of the network in the face of species loss, simulations of sequential host node removal were implemented following established methodologies in network ecology (Albert and Barabási 2002; Dunne *et al.* 2002; Marsiglia *et al.* 2025). Three removal strategies were tested: (i) Removal by centrality: nodes are removed in descending order of betweenness centrality (BC), simulating the selective loss of species with the greatest role as structural connectors—analogous to a targeted attack on key nodes (Albert and Barabási 2002). (ii) Removal by degree: nodes are removed in descending order of degree (k), simulating the preferential loss of hosts that harbor the greatest epiphytic richness. (iii) Random removal: nodes are removed in random order, simulating untargeted disturbances. This scenario was repeated 1,000 times to estimate the average distributions standard deviation, a statistically sufficient number of replicates to stabilize the estimates of the mean and variance under random permutation (Good 2000; Manly 2006).

At each removal step, two structural integrity metrics were calculated on the largest connected component remaining (Newman 2010): (i) Relative size of the LCC ( ): proportion of nodes in the largest component relative to the initial total (383 nodes); LCC values < 0.5 indicate severe network fragmentation. (ii) Average Length of the Shortest Path (APL): average of the geodesic distances between all pairs of reachable nodes in the largest component; abrupt increases indicate degradation of overall connectivity. The removal process continued until all host nodes were eliminated. Robustness was evaluated by plotting the trajectory of LCC and APL against the cumulative percentage of hosts removed. All simulations were implemented with custom functions in R based on the igraph package (Csárdi *et al.* 2023).

Niche Overlap Analysis

The functional complementarity between pairs of hosts was evaluated using the Jaccard Similarity Index for their sets of associated epiphytes (Jaccard 1908). For hosts “a” and “b”, the index is calculated as:

$$J(A,B) = \frac{|E_a \cap E_b|}{|E_a \cup E_b|}$$

Where E_a and E_b are the sets of epiphytes associated with hosts “a” and “b”, respectively. A value of 0 indicates completely disjoint sets (maximum complementarity, zero redundancy), and a value of 1 indicates identical sets (maximum redundancy, zero complementarity).

To test the hypothesis that central hosts (key engineers) harbor more unique sets of epiphytes, the set of hosts was divided into two groups according to their intermediary centrality (CB): high centrality (upper quartile, percentile ≥ 75) and low centrality (lower quartile, percentile ≤ 25). This threshold of extreme quartiles, widely used in network ecology studies to maximize contrast between groups (Jordano *et al.* 2003; Olesen *et al.* 2007), allowed us to identify hosts with clearly differentiated structural functions. The average Jaccard similarity was calculated for all possible pairs within each group. The significance of the difference between the means was assessed using a nonparametric Monte Carlo permutation test (Manly 2006). In each of the 1,000 permutations, the labels of "high" and "low" centrality were randomly reassigned among the hosts, maintaining the original group sizes, and the difference in means was recalculated. The p-value was calculated as the proportion of permutations in which the absolute difference between means was equal to or greater than the observed. Similarity calculations were implemented using the vegan v2.6-4 package (Oksanen *et al.* 2019).

Rationale for the Proxy Approach and Distribution Inference Model

Given that direct data on habitat distribution is not available for most of the hosts included in the database, an indirect inference approach was implemented based on information contained in their associated epiphytes (matrix H). This approach is based on the ecological premise that epiphytic macroalgae, depending on the living substrate provided by the host, record in their habitat distribution a faithful trace of the habitats frequented by the host (co-occurrence fidelity hypothesis) (Simberloff and Dayan 1991; Krasnov *et al.* 2004). This principle is analogous to the use of indicator or companion species as proxies for environmental conditions in biogeography and community ecology (Dufrêne and Legendre 1997). The approach is particularly justified in epiphyte-host systems in marine ecosystems, where physical association implies shared exposure to the abiotic conditions of the habitat.

To infer the potential distribution of hosts across habitats, we applied a simple threshold-based model. For a given host k, let E_k be the set of epiphyte species recorded on that host. The host was considered present in a habitat h if at least 30% of its associated epiphytes were documented in that habitat:

$$\text{Host } k \text{ present in a habitat } h \text{ if } \frac{\sum_{j \in E_k} H_{jh}}{|E_k|} \geq \tau$$

The optimal threshold τ=0.30 was calibrated by cross-validation with a subset of 18 hosts of known distribution, maximizing sensitivity (0.85) and specificity (0.82).

Subsequently, to incorporate uncertainty and habitat and host-specific effects, a hierarchical Bayesian model was specified. The latent variable (Z_{kj}) indicates the presence of host k in habitat j and was modeled as:

$$Z_{kj} \sim Bernoulli(\theta_{kj})$$

Where:

$$\theta_{kj} = logit^{-1}(\alpha_j + \beta_k + \gamma_{kj})$$

$$\alpha_j \sim Normal(\mu_\alpha, 1), \qquad \mu_\alpha \sim Normal(0,1)$$

$$\beta_k \sim Normal(0, \sigma_\beta), \qquad \sigma_\beta \sim Cauchy(0,2)$$

$$\gamma_{kj} \sim Normal(0,1), \qquad \sigma_\gamma \sim Cauchy(0,1)$$

The components of the model represent: α_j: specific effect of habitat *j*; β_k: specific effect of host k; γ_{kj}: host-habitat interaction term

Inference was performed with Stan v2.32.3 via the rstan v2.32.3 package (Carpenter *et al.* 2017; Stan Development Team 2025), using 4 MCMC chains with 4000 iterations per chain (2000 warm-up). Convergence of the chains was verified using Gelman-Rubin's $\hat{R}$ statistic ($\hat{R} < 1.10$ for all parameters) and effective sample sizes (ESS > 1000), thresholds recommended to ensure reliable posterior inference (Vehtari *et al.* 2017). The model was validated with the same subset of 18 hosts of known distribution (Accuracy = 0.83, F1-score = 0.84).

Modeling Epiphytic Richness

Epiphytic richness for host i was defined as the total number of associated epiphytes. Two predictor variables were included, both standardized to z-scores to facilitate comparison of effects (Gelman and Hill 2006). The first variable was the inferred habitat breadth (x_{1i}) given by the number of habitats where host *i* is present according to the inference model in step *1*. The second variable included was the intermediation centrality (x_{2i}) consisting of the value of C_B (*v*) for the node corresponding to host *i*.

As a preliminary analysis, four frequentist statistical models were evaluated: (1) Poisson GLM, (2) Negative Binomial GLM, (3) Quasi-Poisson GLM, and (4) quantile regression, with selection using AIC (Burnham and Anderson 2002; Zhang *et al.* 2023) and residual diagnosis. After

detecting significant overdispersion in the Poisson GLM (variance/mean ratio > 3), a complete Bayesian modeling with Negative Binomial distribution was performed, implemented with the brms v2.20.4 package (Bürkner 2017, 2018).

The complete specification of the Bayesian model was:

$$y_i \sim \text{NegativeBinomial}(\mu_i, \emptyset)$$

$$log(\mu_i) = \beta_0 + \beta_1 x'_{1i} + \beta_2 x'_{2i}$$

$$\beta_0 \sim \text{Normal}(1,2)$$

$$\beta_1, \beta_2 \sim \text{Normal}(0,0.5)$$

$$\emptyset \sim \text{Gamma}(2,1)$$

Where: μ_i: expected mean epiphytic richness for host I; ϕ: dispersion parameter (inverse of the overdispersion parameter) and x_{1i}, x_{2i}: standardized predictors.

The convergence diagnosis of the MCMC chains was performed using the bayesplot v1.10.0 package (Gabry *et al.* 2019), verifying $\hat{R} < 1.10$ and ESS > 1000 for all parameters (Vehtari et al., 2021). Predictive validation included: (i) posterior predictive checks to assess the distributional adequacy of the model and (ii) leave-one-out cross-validation with the PSIS-LOO estimator (loo package v2.6.0) (Vehtari *et al.* 2017). Multicollinearity among predictors was assessed using the variance inflation factor (VIF < 5; car package v3.1-2) (Fox and Weisberg 2018). Overall goodness of fit was also assessed using the *eperformance* package v0.10.8 (Lüdecke *et al.* 2021). The entire Bayesian modeling process was implemented using the rstan v2.32.3, brms v2.20.4, bayesplot v1.10.0, loo v2.6.0, and rstanarm v2.32.1 packages (Muth *et al.* 2018).

Development of the Integrated Vulnerability Index

To translate ecological findings into an applicable conservation prioritization tool, a composite index was developed that integrates habitat vulnerability and network structural vulnerability, explicitly considering the role of species as ecosystem engineers (Sanders and Frago 2024) and as highly connected nodes (Guimarães 2020).

The vulnerability of Cuba's main marine habitats (coral reefs, seagrass beds, mangroves, and soft bottoms) was assessed using an original Marine Habitat Vulnerability Composite Index (ICVHM). The CMHVI is structured around the IPCC (Pörtner *et al.* 2022) conceptual framework for vulnerability assessment, which breaks vulnerability down into three components: sensitivity, exposure, and adaptive capacity (or resilience). This framework is the international standard for coastal vulnerability assessments (Ellison 2015; Pörtner *et al.* 2022) . For each

habitat, ordinal values from 1 to 5 were assigned for each component: sensitivity (S), exposure (E), and resilience (R), based on ecological criteria and regional empirical data (Micheli *et al.* 2013; Villamizar and Cervigón 2017; Valderrama *et al.* 2018; Pina-Amargós *et al.* 2023). The values assigned to each component are shown in the Supplementary Material (Table S1).

The resilience component was re-expressed as (5 − R) so that higher values reflect greater vulnerability, following the standard convention that lower adaptive capacity contributes positively to the total vulnerability of the system (Halpern *et al.* 2008; Keyes *et al.* 2021). The resulting formula integrates the three components into a normalized 1–5 scale. The resilience component was re-expressed as (5 − R) so that higher values reflect greater vulnerability, following the standard convention that lower adaptive capacity contributes positively to the total vulnerability of the system (Halpern *et al.* 2008; Keyes *et al.* 2021). The resulting formula integrates the three components on a normalized 1–5 scale:

$$Vhab = \frac{S + E + (5 - R)}{3}$$

This approach normalizes the vulnerability of each habitat on a scale from 1 (minimum) to 5 (maximum), facilitating comparisons between habitat types. The selection of values was based on regional and global scientific literature on the status, threats, and ecological responses of tropical coastal systems (Micheli *et al.* 2013; Ellison 2015; Pörtner *et al.* 2022).

Secondly, the network vulnerability ($V_{network}(k)$) was calculated. For each host k, an index was calculated that combines its degree (epiphyte richness) and betweenness centrality (role as a structural connector), scaled to a range of 1-5 to be comparable with V_{hab}. This index reflects the importance of the host as an ecosystem engineer within the network of interactions according to the following equation:

$$V_{network}(k) = \frac{1}{2}\left(\frac{k}{k_{max}} + \frac{C_B}{C_{Bmax}}\right) \times 5$$

Where k_{max}= 118 and C_{Bmax}= 0.379 are the maximum values observed in the network (corresponding to *Rhizophora mangle*).

The Integrated Community Vulnerability Index ($V_{total}(c)$) was calculated for each modular community c identified by the Louvain algorithm as an integrated vulnerability value that considers both the environmental context (habitat) and the most critical structural component (the key engineer) within the community:

$$V_{total}(c) = \frac{V_{hab}(c) + V_{network\ max}(c)}{2}$$

Where $V_{hab}(c)$ is the average (weighted by the number of hosts) of the V_{hab} scores of the main habitats where the hosts of community "c" are found; $V_{networkmax}$ (c) is the maximum value of Vnetwork (k) among all hosts belonging to community c, linearly scaled to the range 1-5. This index allows us to evaluate the vulnerability of a modular community dominated by its most structurally important engineer species, whose loss could trigger disproportionate changes. This index V_{total} varies between 1 and 5, where higher values indicate modular communities with higher conservation priority, combining high exposure to environmental threats with a critical dependence on structurally irreplaceable host species that act as key engineers and network connectors.

Data and Code Availability Statement

All data generated or analyzed during this study are included in this published article supplemental information files. The primary datasets (habitat interaction matrices) are available on Figshare (Jover, Guerrero, Machell, A M Suárez, and Pérez-Llorens 2026). The complete analytical results, including inferred distributions, network metrics, and model results, are available on Figshare (Jover, Guerrero, Suárez, *et al.* 2026). The R code to reproduce all analyses is archived in Zenodo (Jover and Cabrera 2026) and actively maintained on GitHub (https://github.com/AJoverCapote/EpiphyteHost-Cuba-Analysis). All components are integrated into a Figshare collection (Jover, Guerrero, Machell, Ana M Suárez, and Pérez-Llorens 2026).

RESULTS

Architecture of the epiphyte–host interaction network

The epiphyte–host interaction network of Cuban coastal marine ecosystems comprised 396 nodes and 1,089 edges (Fig. 2A). The node set included 130 host taxa and 266 epiphytic macroalgal species with at least one documented interaction. Global network metrics (Table 1) indicated low connectance (D = 0.0315). The average path length (APL) was 3.44, the network diameter was 9, and the global clustering coefficient was zero, suggesting the absence of transitivity at the network scale.

The degree distribution of the complete network showed a significantly better fit to the truncated power-law model (AIC = −8.52, AIC weight = 99.9%) than to either the exponential model (ΔAIC = 13.87, AIC weight = 0.1%) or the pure power law (ΔAIC = 34.92, AIC weight ≈ 0%). The host degree distribution was markedly right-skewed (Fig. 2B, 2C).

The ten hosts with the highest epiphytic richness accounted for 42.2% of all recorded interactions (Table 2). *Rhizophora mangle* L. had the greatest epiphytic richness (118 epiphytes, *C*B = 0.379) and also exhibited the highest values of both betweenness and closeness centrality. *Digenea simplex* (Wulfen) C. Agardh and *Thalassia testudinum* K.D. Koenig each harbored 58 epiphytic species, followed by *Palisada perforata* (Bory) K.W. Nam (51 species) and *Stypopodium zonale* (J.V. Lamouroux) Papenfuss (43 species).

Modular organization and community structure

Community detection using the Louvain algorithm identified 18 modules with a global modularity of $Q = 0.424$. Module composition was highly heterogeneous (Fig. S1). Community M1 was the largest, comprising 40 hosts and 32 epiphytic species, followed by C5 (18 hosts, 44 epiphytes), C6 (13 hosts, 46 epiphytes), and C9 (12 hosts, 59 epiphytes). Seven communities (C10, C11, C13, C15–C18) consisted of a single host associated with between 1 and 3 epiphytic species (Fig. 2A; Table S2). Community C9, with 12 hosts, accumulated the highest epiphytic richness (59 species). Single-host communities (C10, C11, C13, C15–C18) harbored nearly exclusive epiphyte assemblages, reflecting strong habitat specificity at the local scale.

Inferred host distributions and epiphyte habitat breadth

A threshold-based inference model ($\tau = 0.30$) calibrated on 18 hosts with known distributions successfully assigned habitat distributions to all 130 hosts (Table S3) (accuracy = 1.0, sensitivity = 1.0 for the validation subset). The subsequent Bayesian hierarchical model achieved an overall accuracy of 0.856 (*F*1-score = 0.846), with sensitivity = 0.892 and specificity = 0.827. MCMC chain convergence was satisfactory for all parameters ($\hat{R} < 1.10$; ESS > 1,000; Fig. S3; Table S4). The mean habitat effect ($\mu_\alpha = -0.37$, 95% CI: −1.07, 0.33) indicated moderate variability in baseline detectability across habitat types. The standard deviation of the host-specific effect ($\sigma_\beta = 1.38$, 95% CI: 1.10, 1.71) was substantially larger than that of the host–habitat interaction term ($\sigma_\gamma = 0.26$, 95% CI: 0.009, 0.73) (Table S3).

Epiphyte habitat breadth, derived from matrix H (321 × 8), showed a strong positive skew: 56.4% of species (181 of 321) were restricted to a single habitat type, with a mean breadth of 1.90 (range: 1–7). Five species were recorded across six habitats: *Dictyota caribaea* Hörnig & Schnetter, *Jania capillacea* Harvey, *J. rubens* (Linnaeus) J.V. Lamouroux, *Herposiphonia secunda* (C. Agardh) Ambronn, and *Melanothamnus sphaerocarpus* (Børgesen) Díaz-Tapia &

Maggs. *Amphiroa fragilissima* (Linnaeus) J.V. Lamouroux was the most habitat-generalist species, occurring across seven habitat types (Fig. 3, Table S3).

Ecological determinants of epiphytic richness: Bayesian modeling

Preliminary frequentist models confirmed overdispersion in the epiphytic richness data (variance-to-mean ratio > 3 for the Poisson GLM). Accordingly, a full Bayesian negative binomial model was fitted with two standardized predictors: inferred habitat breadth (x_1) and betweenness centrality (x_2) (Fig. 4A). MCMC convergence was satisfactory for all parameters ($\hat{R} < 1.10$; ESS > 1,000) (Fig. S3). Posterior predictive checks confirmed adequate distributional fit (Fig. 4B). The global habitat intercept (μ_a) had a posterior mean of 0.37 (SD = 0.362). Leave-one-out cross-validation (PSIS-LOO) did not identify any influential observations, and multicollinearity among predictors was low (VIF < 5) (Table S5).

The posterior median for the habitat breadth effect (β_1) was 0.524 (95% CI: 0.343–0.703). The posterior median for the betweenness centrality effect (β_2) was 0.957 (95% CI: 0.664–1.333) (Fig. 4A). Posterior predictive checks confirmed that the model adequately replicated the observed richness distribution across the 130 hosts (mean = 8.4 species) (Fig. 4B).

Niche overlap among hosts: taxonomic similarity of epiphyte assemblages

Overall Jaccard similarity across all host pairs was low (mean = 0.027; median = 0.000; Fig. 5A). Hosts in the high-centrality group (upper quartile of *C*B) showed a mean Jaccard similarity of 0.087 (SD = 0.105; median = 0.060), calculated across 528 pairs (Fig. 5B). In contrast, hosts in the low-centrality group (lower quartile) exhibited a mean Jaccard similarity of 0.007 (SD = 0.084; median = 0.000) across 1,128 pairs (Fig. 5C). The difference between group means was 0.080 ($p < 0.001$, Monte Carlo permutation test with 1,000 iterations) (Table 3). Inter-module Jaccard similarity values were predominantly below 0.2, while intra-module similarity reached up to 0.3 in the largest modules (C1, C6, C9) (Fig. S4).

Structural robustness to host removal

Sequential host-removal simulations under three strategies yielded distinct trajectories of network structural integrity (Fig. 6; Table 4). Removal by betweenness centrality triggered network fragmentation (LCC < 0.5) after eliminating 14.6% of hosts, with an area under the LCC curve (AUC_LCC) of 0.171. Removal by degree (epiphytic richness) induced fragmentation after 16.2% of hosts were removed (AUC_LCC = 0.190). Under random removal, the network maintained LCC > 0.5 until 64.6% of hosts had been eliminated (AUC_LCC = 0.583) (Table 4).

The maximum increase in average path length (APL) was greater under degree-based removal (ΔAPL_max = 3.16) than under betweenness-based removal (ΔAPL_max = 2.53). The first hosts removed under both targeted strategies included *Rhizophora mangle*, *Thalassia testudinum*, *Digenea simplex*, and *Palisada perforata*.

Integrated Vulnerability Index: community-level conservation prioritization

The Marine Habitat Composite Vulnerability Index (MHCVI) assigned environmental vulnerability scores (V_{hab}) to the eight habitat types. Coral reefs received the highest score (4.33), followed by seagrass beds (4.00), mangroves (3.67), and soft-bottom and rocky substrates (approximately 2.3–2.7).

The network vulnerability index (V_{net}) integrated host degree and betweenness centrality into a normalized 1-to-5 scale (Table 5). *Rhizophora mangle* attained the maximum value (V_{net} = 5.0), followed by *Thalassia testudinum* ($V_{net} \approx 4.26$), *Digenea simplex* ($V_{net} \approx 4.07$), and *Palisada perforata* ($V_{net} \approx 3.67$). Hosts with $V_{net} > 2$ represented 3.8% of the total (5 of 130) yet accounted for 30% of all recorded interactions.

Total Vulnerability Index values ($V_{total)}$ across the 18 modules ranged from low to high (Fig. 7). Only Module 9 (mangrove, *R. mangle*-dominated) attained $V_{total} > 4.0$ (Very High priority), while Modules 6, 2, and 5 ranged between 3.0 and 3.2 (High priority). The remaining modules showed intermediate V_total values (Table S6).

A total of 26 host species were identified as ecosystem engineers, concentrated across 7 of the 18 modules (Table S7). Module M9, associated with mangrove habitats and dominated by *R. mangle*, had the highest V_total (4.264). *R. mangle* exhibited both the greatest epiphytic richness (118 species) and the highest betweenness centrality (*C*B = 0.38). Module M6, representative of seagrass ecosystems, contained four ecosystem engineers, with *T. testudinum* as the dominant species. Module M5 had the highest engineer richness (9 species), including representatives of *Sargassum*, *Hypnea*, and *Laurencia*, with a V_{total} of 3.026. The *V*net values for the principal ecosystem engineers were 5.0 (*R. mangle*), 2.689 (*T. testudinum*), and 2.311 (*P. perforata*).

DISCUSSION

Network topology: scale-free architecture and small-world properties

The Cuban epiphyte–host network shows a truncated power-law degree distribution, confirming hypothesis H1. This topology has been documented in plant–pollinator, host–parasite, and food-web networks across terrestrial, freshwater, and marine environments (Dunne *et al.* 2002;

Jordano *et al.* 2003). The truncation reflects biological constraints on the maximum number of interactions a single host can sustain, a pattern reported in tropical forest mutualistic networks (Marjakangas *et al.* 2020). In our network, *Rhizophora mangle* represents this upper limit with 118 associated epiphytes. Critically, the nodes in this network are not ecologically neutral entities: most high-degree, high-centrality hosts such as *R. mangle* and *Thalassia testudinum* correspond to what Wernberg *et al.* (2024) define as ecosystem engineer: organisms whose biogenic structure defines the physical habitat for a wide array of associated taxa. The network topology is therefore not merely an abstract property but a direct reflection of the ecosystem-engineering capacity of these hosts, a perspective further developed by the facilitation cascade framework (Thomsen *et al.* 2018) and documented at the community level for *R. mangle* (Aquino-Thomas *et al.* 2025).

The network also shows small-world properties: low connectance (D = 0.0315) combined with a short average path length (APL = 3.44). These properties allow efficient dispersal of epiphytic propagules across the host community through few intermediate steps. Food webs in seagrass and coral reef systems show similar short path lengths, suggesting that this structural efficiency may be general in coastal marine networks (Feng *et al.* 2026). The zero global clustering coefficient arises from the strictly bipartite structure and has no equivalent in food webs, where omnivory creates triangular connections.

The right-skewed degree distribution, with ten hosts accounting for 47.1% of all interactions, parallels the hub-dominated connectivity found in mycorrhizal networks (Simard *et al.* 2012) and plant–herbivore networks in Mediterranean systems (Fontaine *et al.* 2011). In those systems, hub species act as conduits for nutrient transfer and energy flow. In our macroalgal network, the hubs are structural ecosystem engineers whose three dimensional architecture creates the microhabitat on which epiphytic communities depend (Jones *et al.* 1994; Thomsen *et al.* 2018).

Modularity: habitat-driven compartmentalization

The network showed 18 modules with global modularity Q = 0.424. This value exceeds the threshold of Q > 0.3 considered indicative of biologically meaningful community structure (Newman and Girvan 2004). It is comparable to Q values reported for plant–pollinator networks in fragmented tropical landscapes (Fortuna and Bascompte 2006) and host–parasite networks of coral reef fish (Poulin 2010). Marine food webs typically show lower modularity (Q = 0.15–0.32) due to the higher connectivity of the water column as a dispersal medium (Valls *et al.* 2015).

The large modules (C1, C5, C6, and C9) are associated with generalist hosts that span multiple habitat types, while the seven single-host peripheral modules contain exclusively specialist epiphytic assemblages. This pattern mirrors the nested modular architecture described for plant–animal mutualistic networks, where generalists form a shared core and specialists are confined to the periphery (Bascompte *et al.* 2003; Olesen *et al.* 2007). In terrestrial systems, this architecture buffers extinction cascades by limiting the spread of perturbations between modules (Fortuna and Bascompte 2006).

In our network, however, modularity does not equalise vulnerability across communities. Module C9, dominated by *R. mangle* in mangrove habitats, simultaneously has the highest epiphytic richness (59 species) and the highest integrated vulnerability (V_{total} = 4.264). The loss of the key engineer in this module would therefore produce a concentrated ecological impact not distributed across the network. This result is consistent with Thomsen *et al.* (Thomsen *et al.* 2018), who showed that secondary ecosystem engineer, including epiphytes, enhance inhabitant richness and that their removal has effects exceeding those predicted from trophic cascades alone. Aquino-Thomas and Proffitt (2025) documented this mechanism at a finer scale: in the mangrove systems of Florida, the presence of secondary ecosystem engineer (SFS) such as oysters and sponges on *R. mangle* roots increased epibiont biodiversity significantly, with effects that varied by interaction type (mutualist, commensal, or parasitic). Our network analysis extends this facilitation cascade to an ecosystem-wide scale, positioning *R. mangle* as the critical connector that channels epiphyte diversity across the entire Cuban coastal ecosystem. However, as reviewed by Wernberg *et al.* (2024), mangroves and seagrass meadows are being severely impacted by climate change through sea-level rise, hurricane intensification, and marine heat waves, threatening the very hub species that sustain the structural integrity of this network. Our results show that beyond their well-recognized ecosystem services (coastal protection, blue carbon storage, megafauna's habitat); the loss of this ecosystem engineer would trigger mass secondary extinction of epiphytes, a cryptic biodiversity maintenance service of equal ecological importance.

Epiphytic richness: network position matters more than habitat breadth

Betweenness centrality (β_2 = 0.957) predicted epiphytic richness more strongly than habitat breadth (β_1 = 0.524). This means that a host species' structural role as a connector within the network explains more of its associated diversity than the number of habitats it occupies. The

result agrees with network theory, which predicts that highly central nodes accumulate both direct and indirect interactions (Bascompte and Jordano 2013). It extends this prediction to a marine macroalgal system for the first time.

A similar pattern has been reported in mycorrhizal networks, where central fungal hubs are associated with higher plant species richness through enhanced nutrient transfer (Simard *et al.* 2012). In freshwater stream networks, macroinvertebrate taxa with high centrality tend to support greater parasite richness (Poulin 2010). The convergence of this result across marine, freshwater, and terrestrial systems suggests that network centrality is a general predictor of associated biodiversity. This network-based framework is complementary to niche-based models that identify direct abiotic drivers: Giraldo-Ospina *et al.*(2025) demonstrated that the density of two kelp ecosystem engineer in California is jointly determined by temperature (heat-wave stress), nitrate availability, wave energy, and biotic interactions (urchin grazing), factors that operate at the population level. Together, both approaches suggest that the persistence and biodiversity role of a foundation host is shaped by its physiological tolerances to abiotic conditions and by its strategic position in the interaction network. Betweenness centrality, in this sense, functions as an integrative variable that captures the cumulative outcome of multiple ecological and evolutionary processes that determine a host's suitability as an epiphytic substrate.

The positive effect of habitat breadth is also biologically meaningful. Habitat generalist hosts such as *T. testudinum*, which occupies seagrass, mangrove, and reef habitats, act as landscape connectors that expose their epiphytic communities to multiple colonist pools. This matches the mass effect mechanism in metacommunity theory (Leibold *et al.* 2004), where species from high diversity habitats reach less favourable ones through dispersal along structurally connected hosts. The weaker effect of habitat breadth relative to centrality suggests that much of its influence on epiphytic richness operates through its covariance with network position.

Niche overlap: functional complementarity and specialist assemblages

The overall mean Jaccard similarity (J = 0.027) is low, indicating that most host pairs share almost no epiphytic species. This high functional complementarity is consistent with strong environmental filtering at the host surface level. Marine invertebrate epibiont communities show similar patterns of low overlap (Memmott *et al.* 2004). In freshwater systems, epiphytic diatoms on macrophytes exhibit low compositional similarity, attributed to fine-scale substrate differences among host species (Soininen *et al.* 2018). In terrestrial systems, vascular epiphytes on tropical

trees show limited overlap in their assemblages across host species (Zotz 2016). Aquino-Thomas and Proffitt (2025) further showed that even within a single host species (*R. mangle*), switching from one type of secondary ecosystem engineer (SFS) to another, e.g. from oysters to sponges, produced epibiont communities with limited compositional overlap. Our results extend this pattern to the whole-host level, indicating that each host species in the Cuban system constitutes a distinct, non-redundant microhabitat, such that the loss of any host represents a net and irreversible loss of epiphytic biodiversity.

Hosts with high betweenness centrality showed greater pairwise similarity ($J = 0.087$) than those with low centrality ($J = 0.007$; $p < 0.001$). This is the opposite of hypothesis H3. Central hosts share a cosmopolitan core of physiologically tolerant epiphytic species such as *Amphiroa fragilissima, Herposiphonia secunda,* and *Jania rubens*. This shared generalist core is consistent with the nestedness architecture documented in plant–animal mutualistic networks, where generalist species form the network's core and specialists are asymmetrically attached to them (Bascompte *et al.* 2003).

Peripheral hosts with low centrality sustain nearly exclusive epiphytic assemblages ($J \approx 0$), functioning as refugia for specialist species absent from the network's generalist core. The disappearance of these peripheral hosts, while having little effect on global network connectivity, would cause irreversible losses of specialist assemblages that contribute disproportionately to total beta-diversity. This function is analogous to peripheral low-productivity habitats in terrestrial conservation biology, where rare specialist species are concentrated away from the highly connected centres of species distribution.

Structural robustness: the cost of scale free topology

The network fragmented after removing only 14.6% of hosts under targeted removal by centrality, compared to 64.6% under random removal. This asymmetry is a well-known consequence of scale-free topology (Albert and Barabási 2002). In Jianfeng Feng *et al.* (2026) reported fragmentation thresholds under targeted removal across multiple food webs. Our observed threshold is lower, which likely reflects the strictly bipartite structure of epiphyte–host networks: unlike food webs, omnivores and generalist feeders cannot rewire interactions after hub loss, leaving no alternative paths to sustain connectivity.

The first hosts removed under targeted strategies, *R. mangle, T. testudinum, D. simplex,* and *P. perforate*, are structurally irreplaceable. Their removal is equivalent to targeting keystone species

in trophic webs (Power *et al.* 1996). In our system, however, they are engineering keystones: their physical structure creates the microhabitat conditions upon which epiphytic communities assemble (Jones *et al.* 1994). The habitat cascade framework predicts that losing a primary engineering host removes not just the substrate but the entire secondary habitat structure built upon it (Thomsen *et al.* 2018).

Degree based removal caused a larger maximum increase in average path length (ΔAPL_{max} = 3.16) than centrality-based removal (ΔAPL_{max} = 2.53). This means that removing the most connected hosts degrades network communication before it causes fragmentation. In soil food webs, loss of highly connected fungal decomposers similarly increases path length before measurable nutrient cycling declines (de Vries *et al.* 2013). These functional degradation sequences may precede the topological collapse that monitoring programmes would detect, making early warning systems based on network metrics particularly important. Empirical evidence from kelp ecosystems adds a further dimension of concern: Giraldo-Ospina *et al.* (2025) documented that after the 2014–2016 California marine heat wave, *Nereocystis* forests failed to recover even when abiotic conditions (temperature, nutrients) returned to favourable levels, because urchin overgrazing stabilised an alternative deforested state. This hysteresis implies that the network collapse predicted by our removal simulations may be not merely rapid but irreversible on management timescales, if a post-disturbance alternative state becomes entrenched. The fragmentation threshold we identified (14.6% host loss) may therefore represent a conservative estimate of true ecological tipping point.

The vulnerability of the network to targeted removal is ecologically alarming. Caribbean coral reefs are projected to decline substantially by 2100 under high-emission scenarios (H Guzmán *et al.* 2023). This would selectively remove reef-associated hosts such as *Stypopodium zonale*, *Laurencia spp*., and *Sargassum* spp., structurally important species concentrated in specific modules. Progressive replacement of *T. testudinum* meadows by opportunistic algae due to eutrophication (van Tussenbroek *et al.* 2017) would selectively eliminate a high-centrality hub ($V_{net} \approx 4.26$) with consequences equivalent to a targeted attack on module M6.

Ecosystem engineers and the Integrated Vulnerability Index

The 26 ecosystem engineers identified are concentrated in 7 of the 18 modules, confirming hypothesis H5. The concept of an ecosystem engineer, an organism that modulates resource availability by physically modifying its environment (Jones *et al.* 1994), applies directly to these

host species. They create the complex surfaces, chemical gradients, and shade conditions that allow epiphytic communities to establish. The uneven distribution of engineers across modules means that the loss of a module's engineer removes both a structural hub and a physical habitat-forming species simultaneously.

Module M9, dominated by *R. mangle* in mangrove habitats, reached the highest V_{total} (4.264). *R. mangle* simultaneously holds the highest epiphytic richness (118 species), the highest betweenness centrality (C_B = 0.379), and the highest V_{net} (5.0) in the entire network. Mangroves have experienced 30–50% global area loss over the past five decades (Ellison 2015), and Caribbean mangroves face additional pressure from sea-level rise and hurricane intensification (Mcleod *et al.* 2010). Our results add a network-structural dimension to this conservation concern that habitat area metrics alone would not capture. Wernberg *et al.* (2024) further note that mangroves store approximately 1,023 Mg C ha^{-1} of blue carbon, meaning that conservation of *R. mangle*-dominated module M9 would simultaneously protect network integrity, cryptic epiphyte diversity, and climate-relevant carbon stocks, a multi-service outcome that aligns with nature-based solution strategies for ecosystem engineer in the Anthropocene.

Module M5, with nine ecosystem engineers including *Sargassum*, *Hypnea*, and *Laurencia* species (V_{total} = 3.026), shows higher engineer redundancy. Redundancy among functionally similar species can buffer the community against the loss of any single engineer, a mechanism analogous to response diversity in seagrass ecosystems (Reusch *et al.* 2005). However, if all engineers in a module share the same habitat type, as is the case in M5, associated with rocky and exposed substrates, then a coordinated habitat level perturbation could eliminate them simultaneously.

The V_{hab} ranking, coral reefs (4.33) > seagrass beds (4.00) > mangroves (3.67) > soft bottoms (≈ 2.3–2.7), is consistent with independent global vulnerability assessments based on cumulative human impacts (Halpern *et al.* 2008) and with IPCC projections for tropical coastal habitats (Pörtner *et al.* 2022). The integration of V_{hab} with V_{net} into a single V_{total} score identifies conservation priorities that neither metric alone would reveal. Module M9 has high V_{total} not because its habitat is the most exposed, but because its dominant engineer is the most structurally irreplaceable. This prioritisation is independently supported by two lines of evidence. First, Aquino-Thomas and Proffitt (2025) project that tropical SFS (especially sponges, which maintain mutualistic relationships with mangroves) will expand poleward under warming, altering epibiont

community structure in ways that our V_{total} index captures through the high structural irreplaceability of the primary host. Second, the abiotic drivers identified by Giraldo-Ospina *et al.* (2025) for ecosystem engineer persistence, including temperature anomalies, nutrient availability, and disturbance regimes, are precisely the variables underlying the habitat-level vulnerability component (V_{hab}) incorporated in our index, providing empirical validation for our scoring approach across contrasting coastal systems.

Comparison across ecosystem types

The modularity (Q = 0.424) of our network exceeds that of most marine food webs (Q = 0.15–0.32) (Valls *et al.* 2015) but matches values from mycorrhizal networks (Q = 0.35–0.50) (Montesinos-Navarro *et al.* 2012) and plant–pollinator networks in fragmented landscapes (Q = 0.35–0.55) (Librán-Embid *et al.* 2021). Marine food webs are less modular because omnivory and the pelagic dispersal medium connect otherwise separate guilds. In our system, hosts are physically anchored to specific habitat types, imposing clear boundaries on epiphytic colonisation pools.

The mean Jaccard similarity observed in our study is substantially lower than values reported for vascular epiphytes on tropical trees (Zotz 2016) and epiphytic lichens on temperate trees (Klein *et al.* 2021). This may reflect the greater physicochemical heterogeneity of macroalgal host surfaces, arising from differences in polysaccharide composition, biofilm chemistry, and surface rugosity (Potin 2012), compared to bark surfaces of trees. Alternatively, the larger species pool (321 epiphytes) in our database arithmetically reduces pairwise similarity compared to most terrestrial studies.

The robustness asymmetry (random vs. targeted removal ratio) observed in our study is higher than that reported for Atlantic seagrass trophic networks (Valls *et al.* 2015) but comparable to strictly bipartite host–parasite networks of freshwater fish, which also show catastrophic fragmentation under targeted host removal (Poulin 2010). The absence of interaction rewiring in bipartite networks, no epiphyte–epiphyte links exist in our system, eliminates the compensatory paths that make food webs more robust. This structural constraint is shared with plant–pollinator networks (Memmott *et al.* 2004).

Conservation implications

The V_{total} index provides a conservation prioritisation tool that integrates two dimensions often assessed separately: environmental exposure of the habitat and structural irreplaceability of its

dominant host. Applied to the 18 modules, it identifies M9 (mangrove, *R. mangle*-dominated) as the highest priority (V_{total} = 4.264), followed by M7 and M12 (V_{total} > 4.0). Current marine protected area strategies in Cuba and the broader Caribbean have focused primarily on coral reef and seagrass habitats (Micheli *et al.* 2013). Our results show that mangrove systems, specifically those dominated by *R. mangle*, deserve equivalent priority based on network-structural criteria. The results also highlight the disproportionate role of a small number of hosts. Nine hosts with V_{net} > 3.5, representing only 6.9% of the total, account for 44.7% of all recorded interactions. Protecting these nine species would preserve nearly half of the documented epiphyte–host interaction space. Targeted protection of structurally critical hosts, combined with habitat-level management, would be more network efficient than species neutral area based conservation.

CONCLUSIONS

Our findings demonstrate that the epiphyte–host network in Cuban coastal ecosystems exhibits a truncated scale-free architecture that, while facilitating propagule dispersal, incurs significant structural vulnerability to the targeted loss of a few engineer host species. Host betweenness centrality emerged as a stronger predictor of epiphytic richness than habitat breadth, and the extremely low epiphyte compositional overlap among hosts underscores the functional uniqueness of each macroalgal host. The network displays marked asymmetric robustness: it resists random species loss but undergoes rapid fragmentation, with only 14.6% of hosts removed, under targeted elimination of central species such as *Rhizophora mangle*, *Thalassia testudinum*, and *Digenea simplex*. By coupling habitat environmental vulnerability with host structural irreplaceability via the Integrated Vulnerability Index (V_{total}), we identify *R. mangle*-dominated mangroves as the highest conservation priority, not only for their well-documented ecosystem services but for their irreplaceable role as biogenic substrates that sustain cryptic epiphytic biodiversity. Critically, a small subset of hosts (5 species; 3.8% of total) supports nearly half of all recorded interactions, suggesting that targeted protection of these structural engineers, combined with habitat-level management, would be more network-efficient than species-neutral area-based approaches. The analytical framework developed here is publicly archived and readily transferable; its application to comparable datasets from other tropical marine regions would enable valuable cross-regional comparisons of network vulnerability. Future research should extend this approach through dynamic models that simulate habitat change trajectories under

climate scenarios, providing managers with time-explicit vulnerability rankings to establish adaptive conservation priorities on a global scale.

Credit authorship contribution statement

Abdiel Jover: Conceptualization, Methodology, Software, Formal analysis, Investigation, Data Curation, Writing – Original Draft and Writing – Review & Editing. **Asiel Cabrera:** Software, Formal analysis, Investigation, Data Curation and Writing – Review & Editing. **Ana M. Suárez**: Resources, Writing – Review & Editing, Supervision. **John Machell**: Resources, Writing – Review & Editing. **José Lucas Pérez-Lloréns**: Resources, Writing – Review & Editing, Supervision.

Acknowledgments

We extend special thanks to the Doctoral Program in Marine Sciences and Technologies at the University of Cádiz and the Doctoral Program in Environmental Sciences at the University of Oriente for the facilities provided during the course of this work. This research was supported by the projects "Environmental scientific services for the development of sustainable agriculture to face climate change in the eastern region of Cuba" and "Risk mitigation plan for biodiversity and food production to address climate change in the eastern region of Cuba," developed within the framework of the collaboration between VLIR-Belgium and the University of Oriente (Cuba). We also thank the Ibero-American University Association for Postgraduate Studies (AUIP) for funding the doctoral scholarship at the University of Cádiz as part of the Collaborative Doctoral Program in Marine Sciences.

REFERENCES

Aderhold A, Husmeier D, Lennon JJ, Beale CM, Smith VA. **2012**. Hierarchical Bayesian models in ecology: Reconstructing species interaction networks from non-homogeneous species abundance data. *Ecological Informatics* **11**: 55–64.

Ahyong S, Boyko CB, Bernot J, *et al.* 2026. *World Register of Marine Species (WoRMS)*. https://www.marinespecies.org.

Albert R, Barabási AL. **2002**. Statistical mechanics of complex networks. *Reviews of modern physics* **74**: 47.

Álvarez-Álvarez JE, Quiroz-González N, Rodríguez-Muñoz DL, Aguilar-Estrada LG. **2020**. Algas epífitas en Padina durvillei y Padina crispata (Dyctiotaceae, Phaeophyceae) en el Pacífico

tropical mexicano. *Acta Botanica Mexicana* **127**: e1594.

Aquino-Thomas J, Sears SJ, Proffitt CE. **2025**. Biogeographic variation in the impact of predation and secondary foundation species on the recruitment and growth of sessile mangrove prop root communities. *Frontiers in Marine Science* **12**: 1599285.

Bascompte J. **2019**. Mutualism and biodiversity. *Current Biology* **29**: 467–470.

Bascompte J, Jordano P. **2007**. Plant-Animal Mutualistic Networks: The Architecture of Biodiversity. *Annual Review of Ecology, Evolution, and Systematics* **38**: 567–593.

Bascompte J, Jordano P. **2013**. *Mutualistic Networks*. Princeton, NJ: Princeton University Press.

Bascompte J, Jordano P, Melián CJ, Olesen JM. **2003**. The nested assembly of plant–animal mutualistic networks. *Proceedings of the National Academy of Sciences USA* **100**: 9383–9387.

Blondel VD, Guillaume J-L, Lambiotte R, Lefebvre E. **2008**. Fast unfolding of communities in large networks. *Journal of Statistical Mechanics: Theory and Experiment* **2008**: P10008.

Bürkner P-C. **2017**. brms: An R Package for Bayesian Multilevel Models Using Stan. *Journal of Statistical Software* **80**: 1–28.

Bürkner P-C. **2018**. Advanced Bayesian Multilevel Modeling with the R Package brms. *The R Journal* **10**: 395–411.

Burnham KP, Anderson DR (Eds.). **2002**. Advanced Issues and Deeper Insights BT - Model Selection and Multimodel Inference: A Practical Information-Theoretic Approach In: New York, NY: Springer New York, 267–351.

Cabrera A, Garcés-Domínguez K, Jover A. **2024**. Relaciones bipartitas macroalgas epizoicas-cangrejos en lechos de macroalgas en la costa suroriental de Cuba. *Novitates Caribaea* **24**: 37–54.

Carpenter B, Gelman A, Hoffman MD, *et al.* 2017. Stan: A Probabilistic Programming Language. *Journal of Statistical Software* **76**: 1.

Chamberlain S, Szoecs E, Foster Z, *et al.* 2020. *taxize: Taxonomic information from around the web*.

Chollett I, Mumby PJ, Cortés J. **2010**. Upwelling areas do not guarantee refuge for coral reefs in a warming ocean. *Marine Ecology Progress Series* **416**: 47–56.

Csárdi G, Nepusz T, Müller K, *et al.* 2023. igraph for R: R interface of the igraph library for graph theory and network analysis. *Zenodo*.

Díaz S, Fargione J, Chapin III FS, Tilman D. **2006**. Biodiversity Loss Threatens Human Well-Being. *PLOS Biology* **4**: e277.

Diez Y, Jover A, Suárez AM, Gómez LM, Fujii MT. **2013**. Distribution of epiphytic macroalgae on the thalli of their hosts in Cuba. *Acta Botanica Brasilica* **27**: 815–826.

Díez I, Muguerza N, Santolaria A, Ganzedo U, Gorostiaga JM. **2012**. Seaweed assemblage changes in the eastern Cantabrian Sea and their potential relationship to climate change. *Estuarine, Coastal and Shelf Science* **99**: 108–120.

Domínguez-García V, Kéfi S. **2024**. The structure and robustness of ecological networks with two interaction types. *PLOS Computational Biology* **20**: e1011770.

Duarte CM, Agusti S, Barbier E, *et al.* 2020. Rebuilding marine life. *Nature* **580**: 39–51.

Dufrêne M, Legendre P. **1997**. Species assemblages and indicator species: the need for a flexible asymmetrical approach. *Ecological Monographs* **67**: 345–366.

Dunne JA, Williams RJ, Martinez ND. **2002**. Network structure and biodiversity loss in food webs: robustness increases with connectance. *Ecology letters* **5**: 558–567.

Ellison JC. **2015**. Vulnerability assessment of mangroves to climate change and sea-level rise impacts. *Wetlands Ecology and Management* **23**: 115–137.

Feng J, Wan X, Wang R, *et al.* 2026. Mediating role of food web structure in linking diversity to multidimensional stability: Evidence from global marine ecosystems. *Science Advances* **11**: eadv3841.

Fontaine C, Guimarães Jr PR, Kéfi S, *et al.* 2011. The ecological and evolutionary implications of merging different types of networks. *Ecology Letters* **14**: 1170–1181.

Fortuna MA, Bascompte J. **2006**. Habitat loss and the structure of plant–animal mutualistic networks. *Ecology Letters* **9**: 281–286.

Fox J, Weisberg S. **2018**. *An R Companion to Applied Regression*. SAGE Publications.

Freeman L. **1977**. A set of measures of centrality based on betweenness. *Sociometry* **40**: 35–41.

Freeman L, Kleypas J, Miller A. **2013**. Coral Reef Habitat Response to Climate Change Scenarios. *PLOS ONE* **8**: e82404.

Gabry J, Simpson D, Vehtari A, Betancourt M, Gelman A. **2019**. Visualization in Bayesian Workflow. *Journal of the Royal Statistical Society Series A: Statistics in Society* **182**: 389–402.

Gelman A, Hill J. **2006**. *Data Analysis Using Regression and Multilevel/Hierarchical Models*. Cambridge: Cambridge University Press.

Gillespie CS. **2015**. Fitting Heavy Tailed Distributions: The poweRlaw Package. *Journal of Statistical Software* **64**: 1–16.

Giraldo-Ospina A, Bell T, Carr MH, Caselle JE. **2025**. Drivers of spatiotemporal variability in a marine foundation species. *Ecological Applications* **35**: e3092.

Good P. **2000**. Theory of Permutation Tests BT - Permutation Tests: A Practical Guide to Resampling Methods for Testing Hypotheses In: Good P, ed. New York, NY: Springer New York, 201–214.

Gossard DJ. **2024**. Syncopation and synchrony: Phenological dynamics of Pyropia nereocystis (Bangiophyceae) in central California. *Journal of Phycology* **60**: 710–723.

Gouveia C, Móréh Á, Jordán F. **2021**. Combining centrality indices: Maximizing the predictability of keystone species in food webs. *Ecological Indicators* **126**: 107617.

Granata A, Abbruzzo A, Patti B, Cuttitta A, Torri M. **2024**. A hierarchical Bayesian model to monitor pelagic larvae in response to environmental changes. *Environmental and Ecological Statistics* **31**: 865–892.

Gribben PE, Kimbro DL, Vergés A, *et al.* 2017. Positive and negative interactions control a facilitation cascade. *Ecosphere* **8**: e02065.

Guimarães PR. **2020**. The Structure of Ecological Networks Across Levels of Organization. *Annual Review of Ecology, Evolution, and Systematics* **51**: 433–460.

Guiry MD, Guiry GM. **2024**. *Algabase*. www.algaebase.org. 10 Jun. 2024.

Guzmán H, Barnes PAG, Lovelock CE, Engel S. **2023**. Climate scenarios and coral reef survival in the Tropical Eastern Pacific and Caribbean. *Frontiers in Marine Science* **10**: 1135240.

Guzmán O, Mendoza E, van Tussenbroek BI, Silva R. **2023**. Effects of Climate-Change-Related Phenomena on Coastal Ecosystems in the Mexican Caribbean. *Sustainability* **15**: 12042.

Halpern BS, Walbridge S, Selkoe KA, *et al.* 2008. A Global Map of Human Impact on Marine Ecosystems. *Science* **319**: 948–952.

Hanley ME, Firth LB, Foggo A. **2024**. Victim of changes? Marine macroalgae in a changing world. *Annals of Botany* **133**: 1–16.

Harder T. **2008**. Marine Epibiosis: Concepts, Ecological Consequences and Host Defence In: Flemming H, Sriyutha P, Venkatesan R, Cooksey K, eds. *Marine and Industrial Biofouling*. Berlin: Springer, 219–231.

Jaccard P. **1908**. Nouvelles recherches sur la distribution florale. *Bulletin de la Société Vaudoise*

des Sciences Naturelles **44**: 223–270.

Jones CG, Lawton JH, Shachak M. **1994**. Organisms as ecosystem engineers. *Oikos* **69**: 373–386.

Jones CG, Lawton JH, Shachak M. **1996**. Organisms as Ecosystem Engineers BT - Ecosystem Management: Selected Readings In: Samson FB, Knopf FL, eds. New York, NY: Springer New York, 130–147.

Jones C, Zurell D, Wiesner K. **2024**. Novel analytic methods for predicting extinctions in ecological networks. *Ecological Monographs* **94**: e1601.

Jordano P, Bascompte J, Olesen JM. **2003**. Invariant properties in coevolutionary networks of plant–animal interactions. *Ecology Letters* **6**: 69–81.

Jover A, Cabrera A. **2026**. *R code for the analysis of epiphytic macroalgae- host interactions*. https://doi.org/10.5281/zenodo.18676047.

Jover A, Cabrera A, Ramos A, *et al.* 2020. *List of presence records of macroalgae epiphytic and host frequent in the Cuban marine shelf (1900-2019).* https://figshare.com/articles/List_of_presence_records_of_macroalgae_epiphytic_and_host_frequent_in_the_Cuban_marine_shelf_1900-2019_/11733735%0Ahttps://ndownloader.figshare.com/files/21356574.

Jover A, Guerrero A, Machell J, Suárez A M, Pérez-Llorens JL. **2026**. *Dataset Epiphyte-Host Interaction Network of Marine Macroalgae in Cuba*. https://figshare.com/articles/dataset/Dataset_Epiphyte-Host_Interaction_Network_of_Marine_Macroalgae_in_Cuba/31359580.

Jover A, Guerrero A, Machell J, Suárez Ana M, Pérez-Llorens JL. **2026**. *Dataset, R code, and results from the analysis of epiphytic macroalgae-host interactions in the Cuban marine shelf*. https://figshare.com/articles/dataset/Dataset_Epiphyte-Host_Interaction_Network_of_Marine_Macroalgae_in_Cuba/31359580.

Jover A, Guerrero A, Suárez AM, Machell J, Pérez-Lloréns JL. **2026**. *Network data for macroalgal epiphyte-host interactions in the Caribbean: structure, vulnerability, and conservation implications*. https://figshare.com/articles/dataset/Network_data_for_macroalgal_epiphyte-host_interactions_in_the_Caribbean_structure_vulnerability_and_conservation_implications/31625680.

Jover A, Ramos A, Cabrera A, Suárez AM, Machell J, Pérez-Lloréns JL. **2020**. Epiphytic macroalgae and hosts of the marine shelf of Cuba: Current status, composition and diversity. *Regional Studies in Marine Science* **34**: 101108.

Keyes AA, McLaughlin JP, Barner AK, Dee LE. **2021**. An ecological network approach to predict ecosystem service vulnerability to species losses. *Nature Communications* **12**: 1586.

Klein J, Low M, Thor G, Sjögren J, Lindberg E, Eggers S. **2021**. Tree species identity and composition shape the epiphytic lichen community of structurally simple boreal forests over vast areas. *PLOS ONE* **16**: e0257564.

Korlević M, Markovski M, Zhao Z, Herndl GJ, Najdek M. **2021**. Selective DNA and Protein Isolation From Marine Macrophyte Surfaces. *Frontiers in Microbiology* **Volume 12**.

Krasnov BR, Shenbrot GI, Khokhlova IS, Degen AA. **2004**. Flea species richness and parameters of host body, host geography and host 'milieu.' *Journal of Animal Ecology* **73**: 1121–1128.

Leibold MA, Holyoak M, Mouquet N, *et al.* 2004. The metacommunity concept: a framework for multi-scale community ecology. *Ecology Letters* **7**: 601–613.

Levin SA. **1992**. The Problem of Pattern and Scale in Ecology: The Robert H. MacArthur Award Lecture. *Ecology* **73**: 1943–1967.

Li P, Yin J, Li F, *et al.* 2025. Exploring the Role of Keystone Species in Marine Ecosystems: A New Perspective Combining Energy Flow and Ecological Network Analysis. *Ecosystems* **28**: 13.

Librán-Embid F, Grass I, Emer C, Ganuza C, Tscharntke T. **2021**. A plant–pollinator metanetwork along a habitat fragmentation gradient. *Ecology Letters* **24**: 2700–2712.

Lüdecke D, Ben-Shachar M, Patil I, Waggoner P, Makowski D. **2021**. erformance: An R Package for Assessment, Comparison and Testing of Statistical Models. *Journal of Open Source Software* **16**: 3139.

Manly BFJ. **2006**. *Randomization, Bootstrap and Monte Carlo Methods in Biology, Third Edition*. Taylor & Francis.

Marjakangas E-L, Abrego N, Grøtan V, *et al.* 2020. Fragmented tropical forests lose mutualistic plant–animal interactions. *Diversity and Distributions* **26**: 154–168.

Marsiglia N, Bosch-Belmar M, Mancuso FP, Sarà G. **2025**. Epibionts and Epiphytes in Seagrass Habitats: A Global Analysis of Their Ecological Roles. *Sci* **7**: 62.

Mcleod E, Hinkel J, Vafeidis AT, Nicholls RJ, Harvey N, Salm R. **2010**. Sea-level rise

vulnerability in the countries of the Coral Triangle. *Sustainability Science* **5**: 207–222.

Memmott J, Waser NM, Price M V. **2004**. Tolerance of pollination networks to species extinctions. *Proceedings of the Royal Society B: Biological Sciences* **271**: 2605–2611.

Micheli F, Halpern BS, Walbridge S, *et al.* 2013. Cumulative Human Impacts on Mediterranean and Black Sea Marine Ecosystems: Assessing Current Pressures and Opportunities. *PLOS ONE* **8**: e79889.

Montesinos-Navarro A, Segarra-Moragues JG, Valiente-Banuet A, Verdú M. **2012**. The network structure of plant–arbuscular mycorrhizal fungi. *New Phytologist* **194**: 536–547.

Muth C, Oravecz Z, Gabry J. **2018**. User-friendly Bayesian regression modeling: A tutorial with rstanarm and shinystan. *The Quantitative Methods for Psychology* **14**: 99–119.

Newman M. **2010**. *Networks: An Introduction*. OUP Oxford.

Newman MEJ, Girvan M. **2004**. Finding and evaluating community structure in networks. *Physical Review E* **69**: 26113.

Oksanen J, Guillaume F, Friendly M, *et al.* 2019. *Community Ecology Package*. https://cran.r-project.org/web/packages/vegan/vegan.pdf.

Olesen J, Bascompte J, Dupont Y, Jordano P. **2007**. The modularity of pollination networks. *Proceedings of the National Academy of Sciences* **104**: 19891–19896.

Olesen J, Dupont Y, Hagen M, Rasmussen C, Trøjelsgaard K. **2006**. Structure and dynamics of pollination networks: the past, present, and future In: Patiny S, ed. *Evolution of Plant–Pollinator Relationships*. Cambridge University Press, 374–391.

Pina-Amargós F, González-Díaz P, González-Sansón G, *et al.* 2023. Status of Cuban Coral Reefs BT - Coral Reefs of Cuba In: Zlatarski VN, Reed JK, Pomponi SA, Brooke S, Farrington S, eds. Cham: Springer International Publishing, 283–307.

Polis GA, Sears ALW, Huxel GR, Strong DR, Maron J. **2000**. When is a trophic cascade a trophic cascade? *Trends in Ecology & Evolution* **15**: 473–475.

Pörtner H-O, Roberts DC, Tignor M, *et al.* 2022. *IPPC 2022: Climate Change 2022: impacts, adaptation and vulnerability: working group II contribution to the sith assessment report of the intergovernmental panel on climate change*. Cambridge University Press.

Potin P. **2012**. Intimate Associations Between Epiphytes, Endophytes, and Parasites of Seaweeds BT - Seaweed Biology: Novel Insights into Ecophysiology, Ecology and Utilization In: Wiencke C, Bischof K, eds. *Seaweed Biology*. Berlin, Heidelberg: Springer Berlin Heidelberg, 203–234.

Poulin R. **2010**. Network analysis shining light on parasite ecology and diversity. *Trends in Parasitology* **26**: 492–498.

Power ME, Tilman D, Estes JA, *et al.* 1996. Challenges in the Quest for Keystones: Identifying keystone species is difficult—but essential to understanding how loss of species will affect ecosystems. *BioScience* **46**: 609–620.

Qian SS, Craig JK, Baustian MM, Rabalais NN. **2009**. A Bayesian hierarchical modeling approach for analyzing observational data from marine ecological studies. *Marine Pollution Bulletin* **58**: 1916–1921.

Quiroz-González N, Aguilar-Estrada LG, Acosta-Calderón JA, Álvarez-Castillo L, Arriola-Álvarez F. **2023**. Biodiversity of epiphytic marine macroalgae in Mexico: composition and current status. *Botanica Marina* **66**: 181–189.

Reusch TBH, Ehlers A, Hämmerli A, Worm B. **2005**. Ecosystem recovery after climatic extremes enhanced by genotypic diversity. *Proceedings of the National Academy of Sciences of the United States of America* **102**: 2826–2831.

Salland N, Wilding C, Jensen A, Smale D. **2024**. Spatiotemporal variability in population demography and morphology of the habitat-forming macroalga Saccorhiza polyschides in the Western English Channel. *Annals of Botany* **133**: 117–130.

Sanders D, Frago E. **2024**. Ecosystem engineers shape ecological network structure and stability: A framework and literature review. *Functional Ecology* **38**: 1683–1696.

Schoolmaster DR, Zirbel CR, Cronin JP. **2020**. A graphical causal model for resolving species identity effects and biodiversity–ecosystem function correlations. *Ecology* **101**: e03070.

Simard SW, Beiler KJ, Bingham MA, Deslippe JR, Philip LJ, Teste FP. **2012**. Mycorrhizal networks: Mechanisms, ecology and modelling. *Fungal Biology Reviews* **26**: 39–60.

Simberloff D, Dayan T. **1991**. The Guild Concept and the Structure of Ecological Communities. *Annual Review of Ecology and Systematics* **22**: 115–143.

Soininen J, Heino J, Wang J. **2018**. A meta-analysis of nestedness and turnover components of beta diversity across organisms and ecosystems. *Global Ecology and Biogeography* **27**: 96–109.

Stan Development Team. **2025**. RStan: the R interface to Stan.

Suárez AM, Martínez-Daranas B, Alfonso Sánchez Y, Moreira-González ÁR, Jover Capote A. **2023**. Lista actualizada de las macroalgas marinas cubanas. *Acta Botanica Mexicana*: e2196.

Teagle HH, Hawkins SJ, Moore PJ, Smale DA. **2017**. The role of kelp species as biogenic

habitat formers in coastal marine ecosystems. *Journal of Experimental Marine Biology and Ecology* **492**: 81–98.

Thompson JN. **2006**. Mutualistic webs of species. *Science* **312**: 372–373.

Thomsen MS, Altieri AH, Angelini C, *et al.* 2018. Secondary foundation species enhance biodiversity. *Nature Ecology and Evolution* **2**: 634–639.

Trifonova N, Duplisea D, Kenny A, Tucker A. **2014**. A Spatio-temporal Bayesian Network Approach for Revealing Functional Ecological Networks in Fisheries BT - Advances in Intelligent Data Analysis XIII In: Blockeel H, van Leeuwen M, Vinciotti V, eds. Cham: Springer International Publishing, 298–308.

van Tussenbroek BI, Hernández Arana HA, Rodríguez-Martínez RE, *et al.* 2017. Severe impacts of brown tides caused by Sargassum spp. on near-shore Caribbean seagrass communities. *Marine Pollution Bulletin* **122**: 272–281.

Tylianakis JM, Laliberté E, Nielsen A, Bascompte J. **2010**. Conservation of species interaction networks. *Biological Conservation* **143**: 2270–2279.

Valderrama SP, Ávila AH, Méndez JG, *et al.* 2018. Marine protected areas in Cuba. *Bulletin of Marine Science* **94**: 423–442.

Valls A, Coll M, Christensen V. **2015**. Keystone species: toward an operational concept for marine biodiversity conservation. *Ecological Monographs* **85**: 29–47.

Vehtari A, Gelman A, Gabry J. **2017**. Practical Bayesian model evaluation using leave-one-out cross-validation and WAIC. *Statistics and Computing* **27**: 1413–1432.

Villamizar E, Cervigón F. **2017**. Variability and sustainability of the Southern Subarea of the Caribbean Sea large marine ecosystem. *Environmental Development* **22**: 30–41.

de Vries FT, Thébault E, Liiri M, *et al.* 2013. Soil food web properties explain ecosystem services across European land use systems. *Proceedings of the National Academy of Sciences* **110**: 14296–14301.

Wernberg T, Thomsen MS, Baum JK, *et al.* 2024. Impacts of Climate Change on Marine Foundation Species. *Annual Review of Marine Science* **16**: 247–282.

White PA, Gelfand AE, Frye H, Silander JA. **2024**. Good modelling practice in ecology, the hierarchical Bayesian perspective. *Ecological Modelling* **496**: 110847.

Wiens JJ, Donoghue MJ. **2004**. Historical biogeography, ecology and species richness. *Trends in Ecology & Evolution* **19**: 639–644.

Zhang J, Yang Y, Ding J. **2023**. Information criteria for model selection. *WIREs Computational Statistics* **15**: e1607.

Zotz G. **2016**. *Plants on Plants – The Biology of Vascular Epiphytes*. Cham, Switzerland: Springer International Publishing.

LIST OF FIGURES

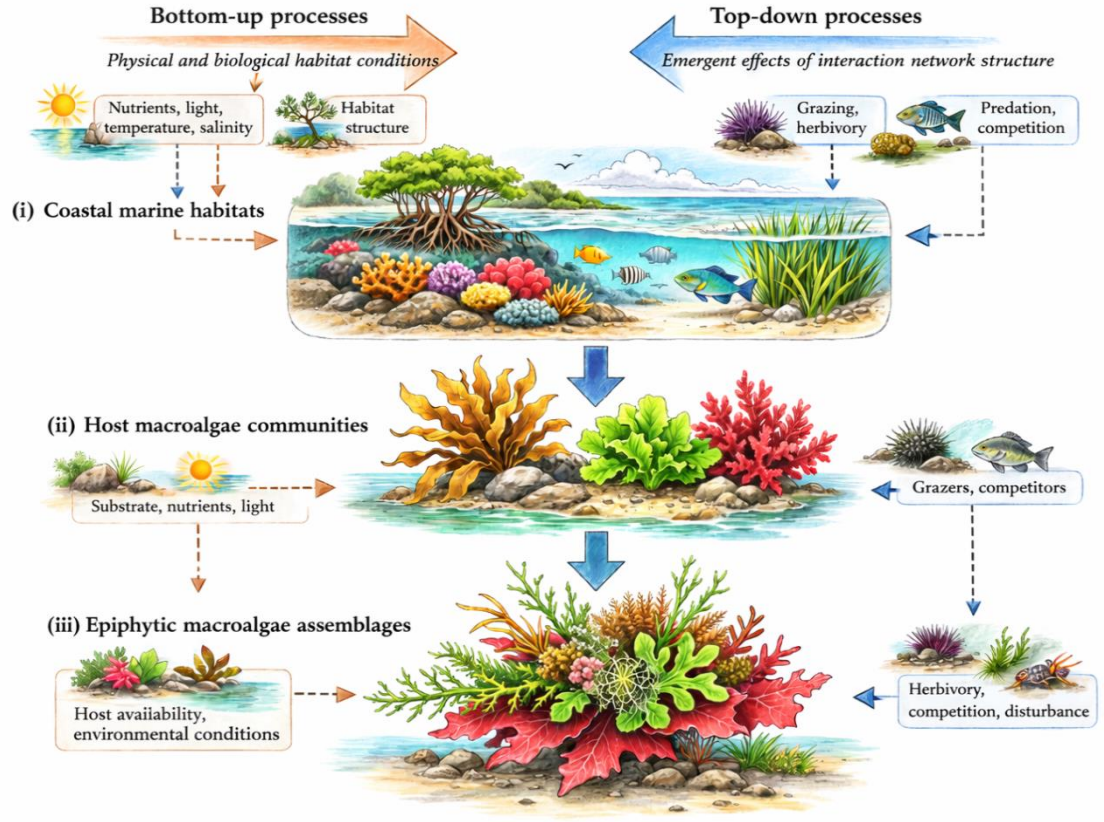

Fig. 1. ***Hierarchical and multiscale conceptual framework of epiphytic macroalgae–host associations in coastal marine ecosystems.*** The diagram integrates bottom-up processes (left; orange arrows) and top-down processes (right; blue arrows) acting simultaneously across three nested organizational levels: (i) coastal marine habitats, (ii) host macroalgal communities and (iii) epiphytic macroalgal assemblages.

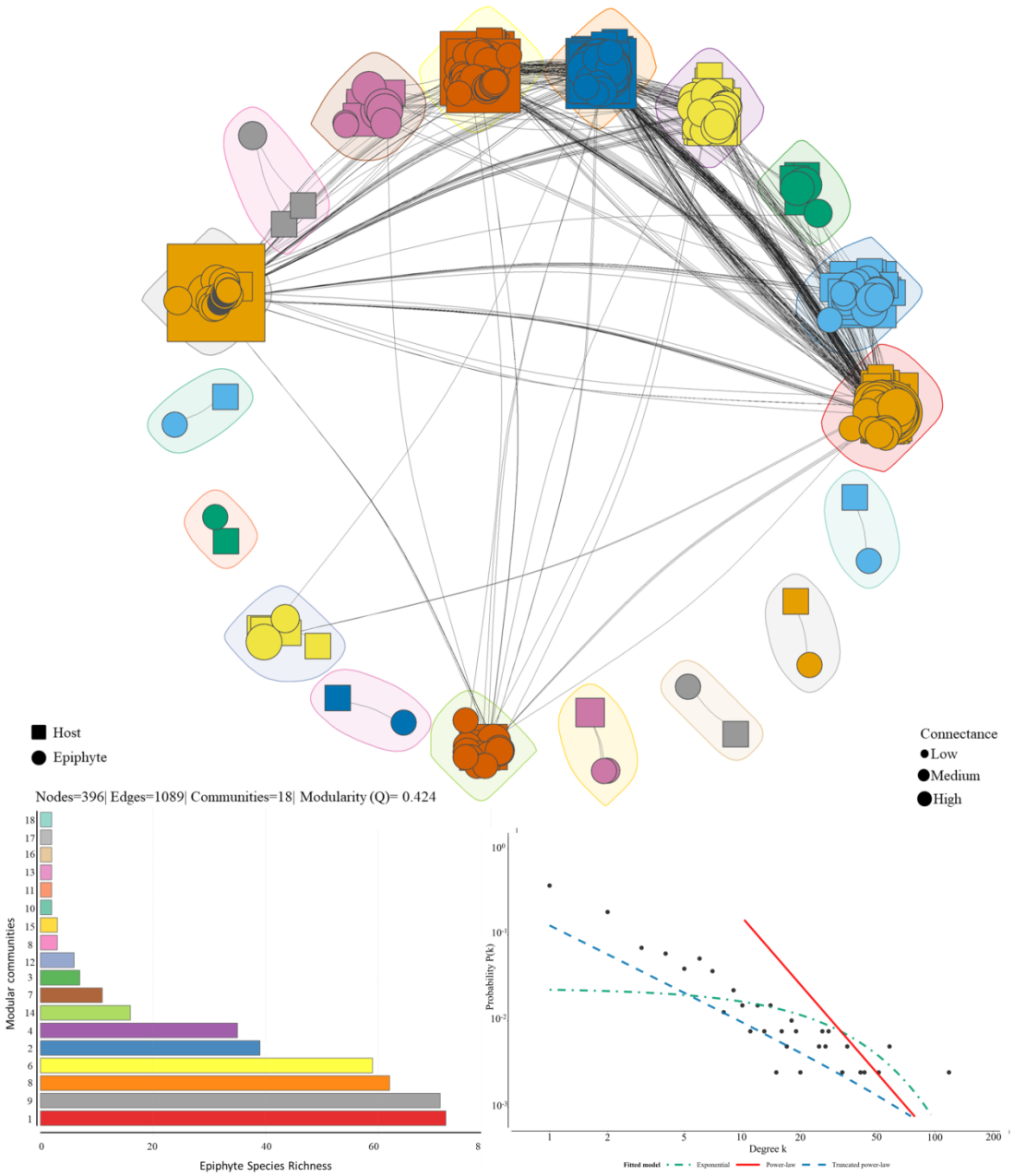

Fig. 2. ***Bipartite epiphytic macroalgae–host interaction network in Cuban coastal marine ecosystems, its modular structure, and degree distribution.*** (A) Full network graph (nodes = 396; edges = 1 089; modularity Q = 0.424; 18 Louvain communities). (B) Species richness per modular community, ordered from community 18 (smallest, n = 2 nodes) to community 1 (largest, n = 72 nodes). (C) Log–log plot of the network degree distribution P(k). Fitted curves: truncated power-law (blue dashed), pure power-law (red solid), exponential decay (green dash-dot). Abbreviations: Q, modularity index (Louvain algorithm, Blondel *et al*. 2008); k, connectivity degree; P(k), probability of degree k.

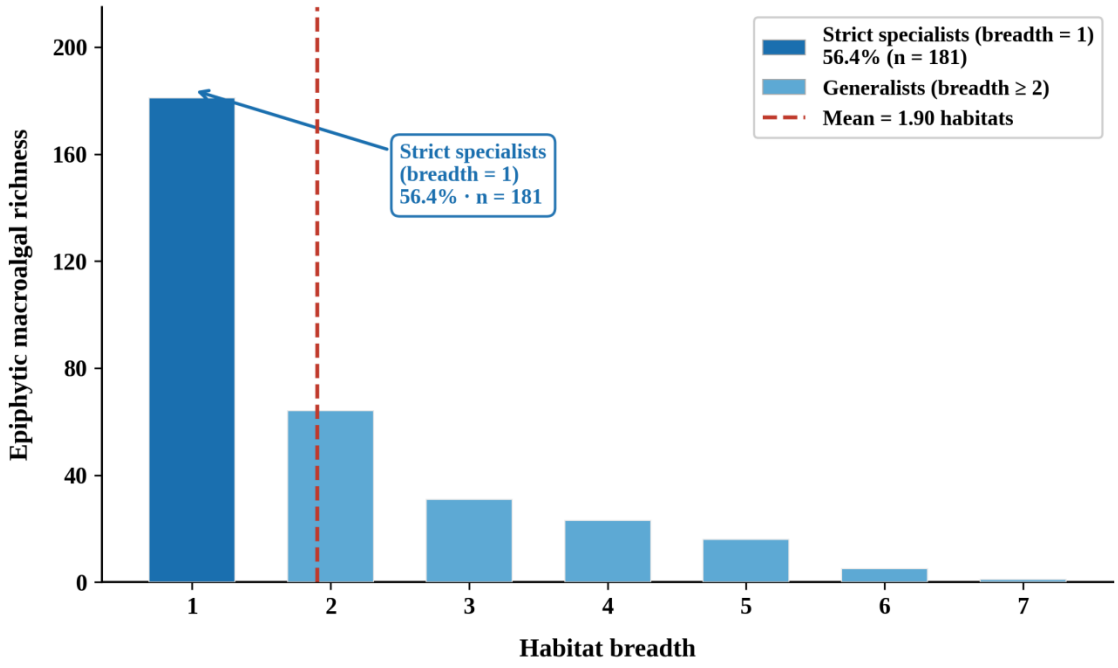

Fig. 3. ***Frequency distribution of habitat breadth among 321 epiphytic macroalgal species across eight Cuban coastal marine habitats.***

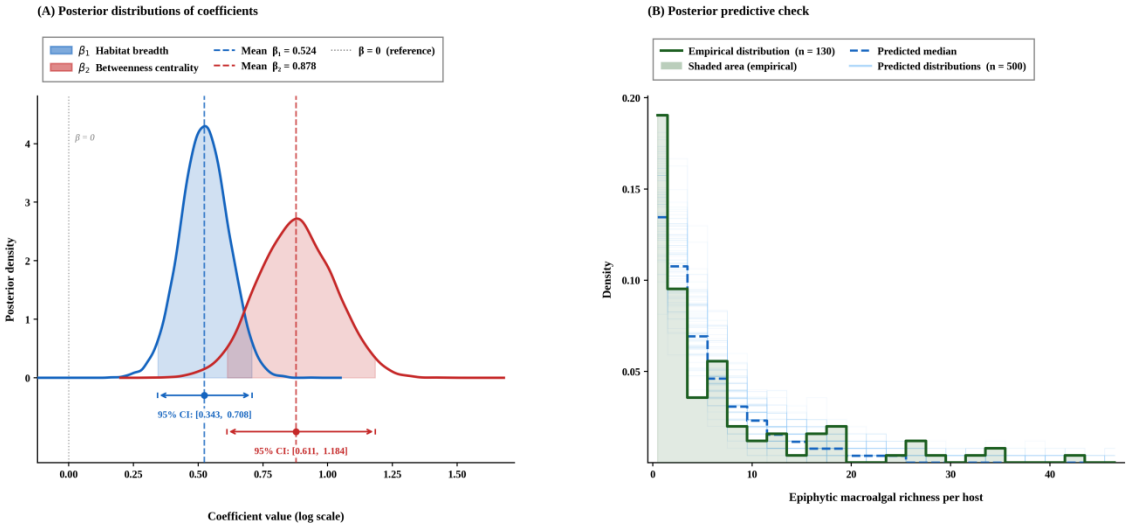

Fig. 4. ***Bayesian negative binomial model results for epiphytic macroalgal richness per host macroalga.*** (A) Posterior distributions of standardized regression coefficients: β_1, habitat breadth (blue); β_2, betweenness centrality (red). (B) Posterior predictive check: the empirical density of epiphytic richness per host (dark green stepped line; shaded area; n = 130) is overlaid on 500 predictive distributions drawn from the posterior (light blue lines) and the predicted median (blue dashed line).

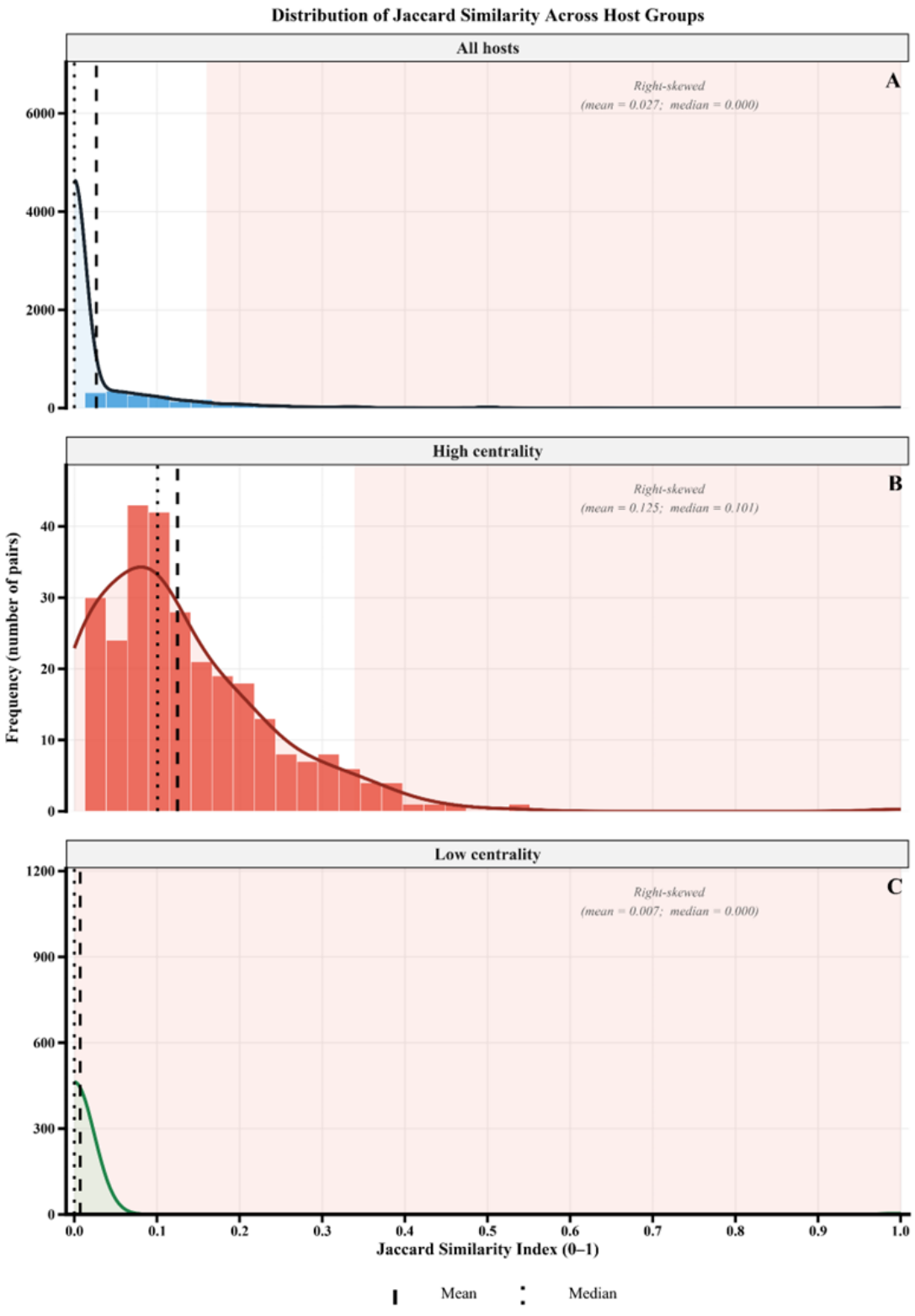

Fig. 5. ***Jaccard similarity distributions across epiphytic macroalgae–host interaction pairs in the Cuban marine macroalgal network, partitioned by host centrality class*****. (A) Global frequency distribution of pairwise Jaccard similarity coefficients (J) for all 8 385 host pairs**

(n = 130 hosts). (B) Jaccard similarity distribution restricted to high-centrality hosts (betweenness centrality C_B > 75th percentile). (C) Jaccard similarity distribution for low-centrality specialist hosts ($C_B \leq$ 25th percentile).

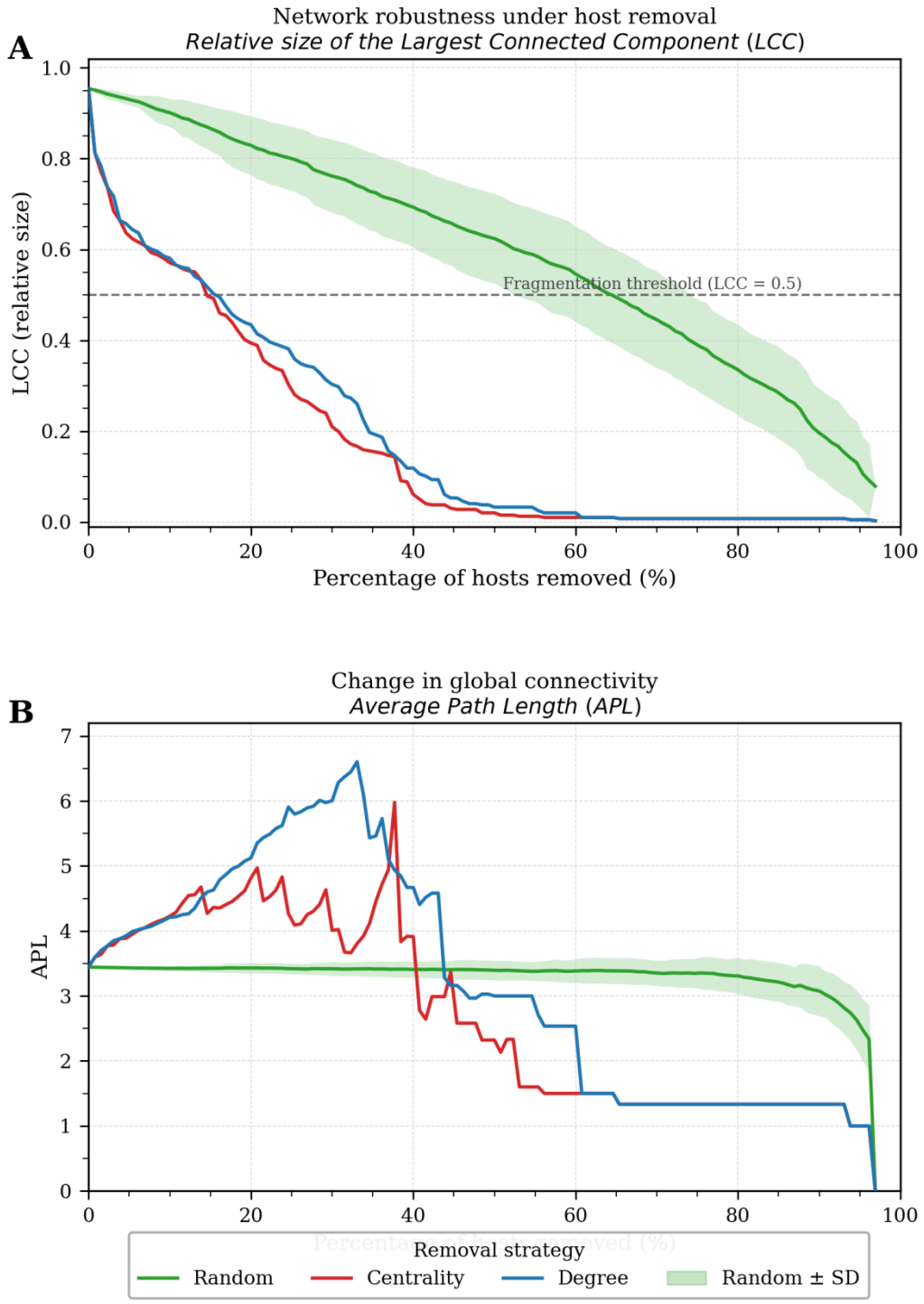

Fig. 6. ***Network robustness of the epiphytic macroalgae–host interaction network under three sequential host-removal strategies*****. (A) Relative size of the Largest Connected Component (LCC) as a function of the percentage of hosts removed. (B) Average Path Length (APL) of the residual largest component as a function of the percentage of hosts removed under the same three strategies. Abbreviations: LCC, largest connected component (expressed as**

fraction of original network size); APL, average path length; SD, standard deviation; k, connectivity degree.

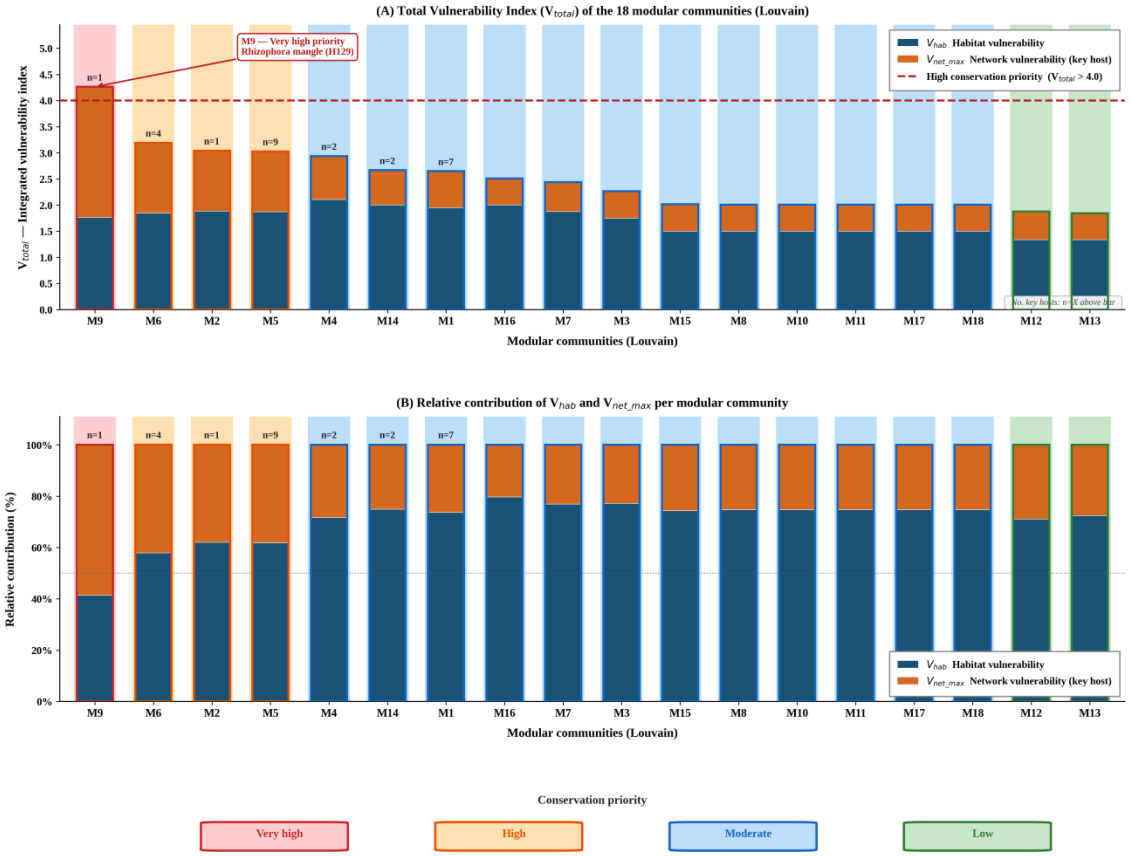

Fig. 7. ***Total Vulnerability Index (V_{total}) and relative component contributions across the 18 Louvain modular communities of the epiphytic macroalgae–host interaction network*.** **Numbers above selected bars indicate the number of ecosystems engineer key hosts (n) identified in that community. (A) Absolute V_{total} values for each community. The horizontal red dashed line marks the V_{total} = 4.0 threshold defining Very High conservation priority. (B) Relative (%) contribution of V_{hab} (dark blue) and V_{net_max} (orange) per community.**

LIST OF TABLES

Table 1. ***Global topology metrics of the epiphytic macroalgae–host bipartite interaction network across coastal marine habitats of Cuba.***

Undirected bipartite network (igraph v1.5.1, R 4.x). APL, average path length; AIC, Akaike Information Criterion; Q, Louvain modularity.

Metric	Value	Ecological interpretation
Network size		
Total nodes (N)	396	130 host + 266 epiphytic macroalgae
Host nodes	130	Macroalgal taxa with ≥ 1 documented interaction
Epiphyte nodes	266	Epiphytic macroalgal species recorded on ≥ 1 host
Edges (interactions)	1 089	Host–epiphyte associations from systematic literature review
Network structure		
Density (D)	0.0315	Sparse network; typical of large bipartite ecological networks
Clustering coefficient	0.000	The global clustering coefficient was zero, as expected by definition for bipartite networks in which triangular paths between nodes of the same partition are structurally precluded
Average path length (APL)	3.44	Short geodesic distance; efficient structural connectivity
Diameter	9	Maximum shortest path between any two nodes
Degree distribution		
Best-fit model	Truncated power-law	AIC weight = 99.9 %; R^2 = 0.629; biologically bounded hubs
vs. Exponential	ΔAIC = +13.87	AIC weight = 0.1 %; moderate fit; does not capture hub structure
vs. Pure power-law	ΔAIC = +34.92	R^2 = −6.30; poor fit
Maximum degree – hosts	118	*Rhizophora mangle*; highest epiphytic richness per host
Maximum degree – epiphytes	41	*Hydrolithon farinosum*; most ubiquitous epiphytic species
Max betweenness centrality	0.379	*Rhizophora mangle*; dominant bridge node of the network
Overdispersion ratio	26.17	The raw data variance-to-mean ratio was 26.17, confirming overdispersion and rendering a standard Poisson GLM inappropriate (residual deviance/df >> 1 in preliminary Poisson GLM
Modular structure		
Modularity Q (Louvain)	0.424	Strong modular structure (Q > 0.3); Blondel et al. 2008
Number of modules	18	Louvain communities; 7 with ecosystem engineer hosts identified
Largest module (C1)	40 hosts / 32 epiphytes	Most species-rich in hosts
Richest module (C9)	12 hosts / 59 epiphytes	Mangrove-dominated; R. mangle as key engineer (V_total = 4.264)

Table 2. ***The ten host macroalgae with the highest epiphytic species richness in the coastal marine interaction network of Cuba.***

k, host degree (number of epiphytic species); C_B, normalised betweenness centrality; C_C, normalised closeness centrality; V_red, network vulnerability index [V_red(h) = V_hab(h) × (1 + k/k_max + C_B/C_B_max)]; k_max = 118, C_B_max = 0.379 (Rhizophora mangle). Species names in italics following international taxonomic conventions.

Rank	Host species	k	C_B	C_C	V_red	Module	Main habitat
1	*Rhizophora mangle*	**118**	0.379	0.449	**5.000**	C9	Mangrove
2	*Digenea simplex*	**58**	0.181	0.410	3.200	C5	Rocky bottom
3	*Thalassia testudinum*	**58**	0.155	0.406	4.264	C6	Seagrass
4	*Palisada perforata*	**51**	0.112	0.393	2.311	C5	Rocky bottom
5	*Stypopodium zonale*	**43**	0.111	0.362	2.313	C2	Rocky bottom
6	*Sargassum polyceratium*	**26**	0.013	0.347	1.517	C5	Rocky bottom
7	*Turbinaria tricostata*	**25**	0.013	0.346	1.483	C5	Rocky bottom
8	*Sargassum buxifolium*	**27**	0.012	0.350	1.517	C5	Rocky bottom
9	*Padina sanctae-crucis*	**35**	0.035	0.359	1.842	C5	Rocky bottom
10	*Alsidium triquetrum*	**19**	0.016	0.326	1.249	C1	Rocky bottom

Table 3. ***Epiphytic niche overlap (Jaccard index) between hosts of high and low betweenness centrality.***

C_B, normalised betweenness centrality; P75, 75th percentile; P25, 25th percentile; J, Jaccard similarity index; SD, standard deviation. Groups were compared using a Monte Carlo permutation test (n = 1 000 iterations; vegan v2.6-4). The high-centrality group comprises 33 hosts (C_B ≥ P75 = 0.0135); the low-centrality group comprises 48 hosts (C_B ≤ P25 ≈ 0).

Group	n pairs	Mean J	SD	Median J	Min	Max	Q1	Q3
High centrality (C_B ≥ P75)	528	0.087	0.105	0.060	0.000	1.000	0.000	0.125
Low centrality (C_B ≤ P25)	1 128	0.007	0.084	0.000	0.000	0.900	0.000	0.000
Difference (High − Low)	—	**0.080**	—	—	—	—	—	—

Note: Monte Carlo permutation test, n = 1 000 iterations; mean difference = 0.080, p < 0.001. C_B, normalised betweenness centrality; J, Jaccard similarity index; SD, standard deviation.

Table 4. ***Structural robustness of the network under sequential host removal using three elimination strategies.***

AUC_LCC, area under the LCC (largest connected component) curve; higher values indicate greater robustness. ΔAPL_max, maximum increase in average path length during removal. Random removal performed with n = 1 000 permutations (mean reported). Initial LCC = 0.955 (fraction of nodes in the main component before removal); initial APL = 3.44. Red/green colours on fragmentation threshold and AUC_LCC indicate high/low vulnerability respectively.

Removal strategy	Fragmentation threshold (%)	AUC_LCC	ΔAPL_max	Initial LCC	Initial APL
Betweenness centrality (directed) *Most vulnerable: network collapse at 14.6 % host removal; critical nodes: R. mangle, T. testudinum, D. simplex, P. perforata.*	**14.6 %**	**0.171**	2.53	0.955	3.44
Degree k (directed) *High vulnerability: loss of degree hubs fragments epiphytic communities at 16.2 % removal.*	**16.2 %**	**0.190**	3.16	0.955	3.44
Random removal (n = 1 000) *Most robust: ~65 % random loss required for fragmentation; scale-free-like architecture confers resilience.*	**64.6 %**	**0.583**	0.00	0.955	3.44

Table 5. ***Total Vulnerability Index (V_total) of the 18 Louvain modular communities of the epiphyte–host network and conservation prioritisation.***

V_hab(c), degree-weighted mean CMHVI of module hosts; V_net_max, maximum network vulnerability index in the module; V_total(c) = [V_hab(c) + V_net_max(c)] / 2. N engineers, number of hosts identified as ecosystem engineers [V_net > P75 and k ≥ module mean; Jones et al. 1994]. CMHVI, Composite Marine Habitat Vulnerability Index (scale 1–5; IPCC AR6 framework). Conservation priorities: Very high (V_total > 4.0), High (3.0–4.0), Moderate (2.0–3.0), Low (< 2.0). Species names in italics.

Module	Conservation priority	N hosts	V_hab(c)	V_net_max	N engineers	V_total(c)	Key engineer host
C9	**Very high**	12	3.528	**5.000**	1	**4.264**	*Rhizophora mangle*
C6	**High**	13	3.692	2.689	4	**3.191**	*Thalassia testudinum*
C2	**High**	13	3.769	2.313	1	**3.041**	*Stypopodium zonale*
C5	**High**	18	3.741	2.311	9	**3.026**	*Palisada perforata*
C4	**Moderate**	11	4.212	1.662	2	**2.937**	*Laurencia intricata*
C14	**Moderate**	2	4.000	1.338	2	**2.669**	*Avrainvillea digitata*
C1	**Moderate**	40	3.900	1.397	7	**2.648**	*Padina gymnospora*
C16	**Moderate**	1	4.000	1.017	0	**2.508**	*Caulerpa racemosa*
C7	**Moderate**	4	3.750	1.128	0	**2.439**	*Gelidiella acerosa*
C3	**Moderate**	4	3.500	1.035	0	**2.267**	*Ruppia maritima*
C15	**Moderate**	1	3.000	1.034	0	**2.017**	*Avrainvillea nigricans*
C8	**Moderate**	2	3.000	1.017	0	**2.008**	*Plocamium cartilagineum*
C10	**Moderate**	1	3.000	1.017	0	**2.008**	*Hypoglossum tenuifolium*
C11	**Moderate**	1	3.000	1.017	0	**2.008**	*Chondria collinsiana*
C17	**Moderate**	1	3.000	1.017	0	**2.008**	*Halimeda incrassata*
C18	**Moderate**	1	3.000	1.017	0	**2.008**	*Boodlea composita*
C12	**Low**	4	2.667	1.085	0	**1.876**	*Grateloupia filicina*
C13	**Low**	1	2.667	1.017	0	**1.842**	*Halymenia floresii*